Computers and Electrical Engineering xxx (xxxx) 110704

Contents lists available at ScienceDirect

Computers and Electrical Engineering

journal homepage: www.elsevier.com/locate/compeleceng

Quality-guaranteed steganographed-MECG signal compression using adaptive truncation of DCT and SVD coefficients and ASCII encoding

Sourav Kumar Mukhopadhyay [a,*], Sridhar Krishnan [b]

[a] School of Computer and Cyber Sciences, Augusta University, 100 Grace Hopper Lane, Augusta, GA 30901, USA
[b] Department of Electrical, Computer, and Biomedical Engineering, Toronto Metropolitan University, 350 Victoria Street, Toronto, Ontario M5B 2K3, Canada

ARTICLE INFO

Keywords:
ASCII character
MECG compression
Optimum DCT
Optimum SVD
Steganography
Quality-guaranteed compression

ABSTRACT

With the proliferation of wearable healthcare devices and garments in the last decade, the necessity of the storage capacity of the acquired biomedical signals; particularly multi-lead electrocardiogram (MECG) signals, and the importance of securing users' personal information have increased significantly. However, existing MECG compression and steganography algorithms are insufficient to address these challenges effectively. This paper presents a discrete cosine transform, singular value decomposition, and American standard code for information interchange (ASCII) character encoding-based highly efficient quality-guaranteed steganographed MECG compression algorithm. The algorithm is tested on three publicly available MECG databases totalling 2.98 months, and its performance is assessed through both qualitative and quantitative measures. The algorithm attains a compression ratio that is much higher than that provided by other algorithms that are developed to compress the MECG signals only. The benefits of using the proposed algorithm are fivefolds: first, the clinical qualities of the reconstructed MECG signals can be controlled precisely, second, user's personal information is restored with no error, third, reconstruction error of the MECG signals is dependent neither on the size of the user's information nor on the steganography operation, fourth, the probability of guesstimating the security-key is close to zero, and fifth, high compression performance.

1. Introduction

Recent advancements in semiconductor fabrication technologies have enabled the acquisition of multi-lead ECG (MECG) signals using compact sensors embedded in smartwatches and garments [1]. By 2025, smartwatch users are expected to reach ~454.69 million globally, and the smart-garment market is projected to reach ~6.7 billion USD annually [2]. With rising interest in personal fitness and healthcare, the demand for MECG recording has grown significantly. While a 12-lead ECG provides comprehensive cardiac insight, it requires ~1.5 MB of memory per minute (1 kHz sampling, 16-bit resolution), which is substantial. Hence, efficient MECG data compression is essential to reduce storage needs without compromising its clinical morphology.

* Corresponding author.
E-mail address: somukhopadhyay@augusta.edu (S.K. Mukhopadhyay).

https://doi.org/10.1016/j.compeleceng.2025.110704
Received 25 February 2025; Received in revised form 17 August 2025; Accepted 6 September 2025
0045-7906/

ECG compression algorithms are generally classified by (i) technique: direct [3], transform-based [4], and prediction-based [5], and (ii) reconstruction quality: lossless [6] or lossy [7]. Each of these direct, transform-based prediction-based methods can be either lossless or lossy and can compress both single and multi-lead ECG signals. However, most of the existing MECG compression algorithms in the literature are transform-based and lossy.

In this present research work, the MECG signals are first denoised and then down-sampled adaptively. Down-sampled MECG signals are arranged to form a two-dimensional (2D) matrix. Next, the 2D discrete cosine transform (DCT) of the matrix is evaluated. Then, singular value decomposition (SVD) of the DCT coefficients is performed. An optimum number of DCT coefficients and singular values are retained dynamically based on a pre-defined quality measure of the MECG signal. Next, the American standard code for information interchange (ASCII) values of the steganographic information are concatenated with the truncated left singular matrix coefficients, and the re-formatted matrix is then compressed using a lossless ASCII character encoding (LL-ACE)-based technique. The right singular matrix coefficients are quantized and then encoded into ASCII characters. Henceforth, we shall call the proposed quality-guaranteed steganographed MECG compression algorithm as *QSMECGcomp* algorithm.

Mukhopadhyay et al. proposed a PPG-based steganography and compression method using SVD and ASCII encoding in [33]. In contrast, this work focuses on ECG signals and introduces several key improvements: (1) an additional DCT-based compression layer alongside SVD and modified ASCII encoding, (2) support for 12-lead ECG instead of single-channel PPG, (3) use of wavelet energy-based diagnostic distortion (WEDD) for quality control, rather than PRD, (4) enhanced ASCII encoding capable of handling values beyond 255, and (5) a more robust and distinct key generation method.

The novelty of the proposed algorithm lies in its ability to: (1) achieve high-performance compression of both ECG and steganographic data, thereby ensuring efficient storage and transmission, (2) precisely control the reconstruction error, which is critical for maintaining diagnostic quality, (3) accurately recover the embedded information, ensuring the integrity and confidentiality of the hidden data, and (4) enhance data security, making it suitable for sensitive medical applications where patient privacy and data protection are paramount. The algorithm's performance is evaluated using both short and long-duration MECG signals from three publicly available online databases with varying sampling rates, totaling a duration of 2.98 months. Such extensive testing demonstrates the algorithm's robustness and scalability across diverse real-world scenarios. The reconstruction error of the MECG signals remains within clinically acceptable limits and never exceeds the predicted error threshold. The algorithm is computationally efficient, exhibiting linear time and space complexities. These features collectively address the limitations of many of the existing MECG compression and steganography techniques and make the algorithm highly suitable for deployment in resource-constrained environments such as wearable devices, portable monitoring systems, or real-time healthcare applications.

The paper is organized as follows. The related research works are presented in Section 2. The proposed *QSMECGcomp* algorithm is presented in Section 3. The reconstruction algorithm of the MECG signals and the restoration technique of patients' confidential information is described in Section 4. The performance of the proposed algorithm is investigated in Section 5. Section 6 compares the performance of the proposed algorithm with that of others. Section 7 analyzes the security of the system. Finally, the algorithm is discussed, and conclusions are drawn in Sections 8 and 9, respectively.

2. Related research works

Several compressive sensing (CS)-based MECG compression methods have been proposed in [8–13]. In [8], an adaptive multi-dictionary CS model exploits the spatial correlations and features of MECG signals. Though claimed to be efficient for wireless body area networks, its high sequential runtime required GPU acceleration. Additionally, its dictionaries are trained on a single dataset, limiting generalizability. In [10], Kronecker-sparsifying bases and the alternating direction method of multipliers (ADMM) method are used for fast reconstruction with acceptable error, but data reduction is suboptimal. Recent tensor decomposition-based approaches [14–16] show promise. In [14], heartbeats are arranged into a tensor and compressed using low-rank CANDECOMP/PARAFAC (CP) decomposition, enabling real-time use. Similarly, Padhy and Dandapat [15] applies discrete wavelet transform and higher-order SVD to the heartbeat tensor, followed by Huffman encoding, offering an efficient multistage compression framework.

In addition to the methods mentioned above, various MECG compression techniques have employed Fourier decomposition [17], principal component analysis [18], wavelet transform (WT) [19,20], and linear prediction [21]. The shared goal of all these methods is not only to save computer memory, but also for bandwidth and power saving in real time tele-healthcare applications.

In clinical practice, alongside MECG signals, demographic and vital signs (e.g., age, gender, blood pressure) are essential for diagnosis and treatment. Ensuring the privacy of such data is mandated by Health Insurance Portability and Accountability Act (HIPAA) [22]. Steganography, i.e., hiding information within a cover signal, has been widely explored for embedding patient data into ECG and other signals [16,23–29,37,40]. Banerjee et al. [16] proposed a tensor decomposition-based MECG compression method that embeds confidential data using higher-order PCA, neural-network-based quantization, and run-length encoding. However, the algorithm does not specify the amount of embedded data or its impact on compression. In [24], an extended binary Golay code achieves lossless recovery of patient data, but it requires user-specific binary matrices, limiting scalability. Abuadbba et al. [25] used the Walsh-Hadamard transform for efficient embedding. Overall, most biosignal steganography techniques suffer from one or more limitations: (1) increased overall data size, (2) signal degradation from processing steps, (3) dependency on the size of hidden data, or (4) potential loss of critical information. Table 1 summarizes the contributions and limitations of several state-of-the-art MECG compression and steganography algorithms compared to the proposed algorithm. As shown in Table 1 and subsequent tables, the proposed algorithm outperforms state-of-the-art algorithms in both compression and steganographic performance.

Table 1
Contributions of several state-of-the-art MECG compression and steganography algorithms.

Algorithm – year	Technique	Compression performance	Steganography performance	Time complexity
[16] - 2021	Tucker Decomposition	Low compared to the proposed algorithm	Not reported	Not mentioned; usually it is non-linear
[9] – 2020	Compressed sensing	Very low; tested only on 5120 × 10 ECG samples	Does not include steganography	Not mentioned; usually it varies between $O(n^2)$ to $O(n^3)$
[17] – 2022	Fourier decomposition	Low compared to the proposed algorithm; reconstruction error always surpasses the predicted value.	Does not include steganography	Not mentioned; Non-linear; usually it varies between $O(M{\cdot}n)$ to $O(M{\cdot}n^2)$; n is number of samples, and M is the number of iterations.
[10] – 2020	Compressed sensing	Very low compared to the proposed algorithm.	Does not include steganography	Fast
[14] – 2021	Tensor decomposition	Low compared to the proposed algorithm; reconstruction error is high.	Does not include steganography	Very high; Non-linear; denoted by $O(T{\cdot}N{\cdot}R{\cdot}I_{prod})$; T is the number of iterations, N is the order of the tensor, R is the rank of the tensor and I_{prod} is the size of the tensor.
[23] – 2022	Particle swarm optimization in Hermite Space	Does not include compression	Low loss of steganographic data	Not mentioned
[24] – 2021	Extended Binary Golay Code	Does not include compression	No loss of steganographic data, but restriction in steganographic data-size and increase in overall data-size.	Linear; $O(n)$
Proposed	DCT, SVD, ASCII character encoding	High compression performance	High data reduction and reconstruction performance even after steganography; no loss of steganographic data.	Linear

3. Material and methods

The proposed *QSMECGcomp* algorithm is divided into five parts: (i) preprocessing, (ii) optimal truncation of DCT coefficients and singular values, (iii) steganography and LL-ACE of the left singular matrix coefficient, (iv) quantization of the right singular matrix coefficient, and (v) generation of the security-key. A block diagram of the proposed *QSMECGcomp* algorithm is shown in Fig. 1.

3.1. Preprocessing

In this study, the 12-lead ECG, i.e., the MECG signals are collected from three publicly available online ECG databases. A 12-lead ECG signal is composed of 3 limb leads (lead I, II, and III), 3 augmented limb leads (lead aVR, aVL and aVF), and 6 precordial leads (lead V1 to V6). Among these 12 ECG leads, four leads (lead III, aVR, aVL and aVF) are linearly correlated to lead I and II. Therefore, these four ECG leads are excluded from processing. Henceforth, MECG refers to eight ECG leads (I, II, V1 –V6) in this article.

Due to its low-frequency nature, ECG signals get routinely corrupted with various sources of high and low-frequency noises during acquisition. Therefore, the elimination of noise from the ECG signal is essential before any other processing. The clinical bandwidth of an ECG signal lies in the range of 0.5–100 Hz. In this research work, each of the eight ECG leads is denoised using 4th order zero-phase Butterworth low-pass and high-pass filters of cutoff frequencies 100 Hz and 0.5 Hz, respectively. For the purpose of perfor-

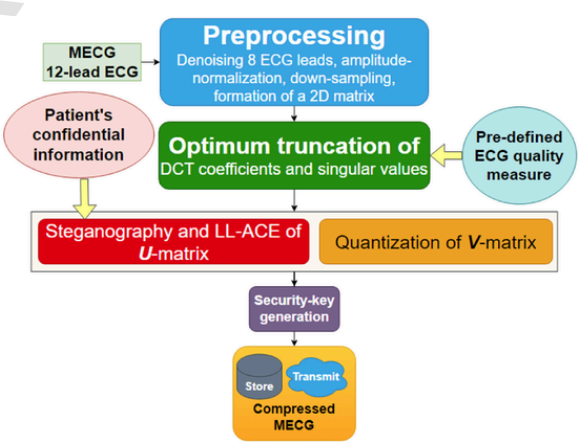

Fig. 1. Block schematic of the proposed *QSMECGcomp* algorithm.

mance evaluation at different stages, these eight denoised ECG leads (voltage values) are stored in a file named 'Original ECG.dat'. Next, the amplitudes of each of these eight denoised ECG leads are normalized to lie within the range of ± 1, and the corresponding eight amplitude-normalization factors (denoted as $ANF_{1 \times 8}$) are stored for later use. Now, each of the amplitude-normalized ECG leads is down-sampled in such a way that the sampling frequency of the down-sampled signal would not be less than 250 Hz. The down-sampling technique used in this study is shown below.

if sampling frequency $> 250Hz$

$D = integer\left(\frac{sampling\ frequency}{250}\right)$

downsample ECG lead I, II, $V1 - V6$ *by D*

end

The down-sampled ECG signals are then arranged to form a 2D matrix following the lead order suggested in [30]. According to [30] the precordial leads should be placed in the first six columns and lead I and II should be placed in the 7th and 8th columns of the matrix, respectively, to exploit the inter and intra lead correlations, that exists among MECG signals, to the fullest extent. The 2D matrix is denoted as $MECG_{r \times 8}$, where r is the number of samples in each lead after down-sampling.

3.2. Optimum truncation of DCT coefficients and singular values

Discrete cosine transform (DCT) has long been used for coding images and metrics. DCT's strong energy compaction property yields its application an ideal in the domain of data compression. The 2D DCT, i.e., DCT-II of a matrix $A_{M \times N}$ is defined as

$$\mathrm{B_{pq}} = \alpha_{\mathrm{p}}\alpha_{\mathrm{q}} \sum_{m=0}^{M-1} \sum_{n=0}^{N-1} \mathrm{A_{mn}} \cos \frac{\pi\,(2\mathrm{m}+1)\,\mathrm{p}}{2\mathrm{M}} \cos \frac{\pi\,(2\mathrm{n}+1)\,\mathrm{q}}{2\mathrm{N}} \tag{1}$$

where $0 \le p \le M-1$ and $0 \le q \le N-1$

$$\alpha_{\mathrm{p}} = \frac{1}{\sqrt{\mathrm{M}}} \text{ for } p = 0 \tag{2}$$

$$\alpha_{\mathrm{p}} = \sqrt{\frac{2}{\mathrm{M}}},\ 0 \le p \le M-1 \tag{3}$$

$$\alpha_{\mathrm{q}} = \frac{1}{\sqrt{\mathrm{N}}} \text{ for } q = 0 \tag{4}$$

$$\alpha_{\mathrm{q}} = \sqrt{\frac{2}{\mathrm{N}}},\ 0 \le q \le N-1 \tag{5}$$

where M and N are the number of rows and columns of the matrix A, respectively, and B is the DCT-II coefficient matrix. In general, DCT tries to concentrate most of the energy of a signal, image, or matrix within the first few coefficients. As a result, the contribution of a large number of DCT coefficients in reconstructing the original data seems to be negligible. These redundant DCT coefficients can be optimally discarded to achieve data compression.

On the other hand, singular value decomposition (SVD) is a technique of matrix factorization and can be mathematically expressed as

$$\mathrm{A}_{M \times N} = \mathrm{U}_{M \times M}\, \mathrm{S}_{M \times N}\, \mathrm{V}^{\mathrm{T}}_{N \times N} \tag{6}$$

The columns of U $\left(\left[u_1, u_2, \ldots, u_M\right]\right)$ matrix are the left singular vectors and are composed of the eigenvectors of AA^T, S is a diagonal matrix which contains the singular values (β) and are the square roots of the eigenvalues either from AA^T or A^TA, and the rows of V^T $\left(\left[v_1, v_2, \ldots, v_N\right]\right)$ matrix are the right singular vectors and are composed of the eigenvectors of A^TA. The singular values, i.e., the diagonal elements of S matrix are real numbers and are arranged in descending order. The total information-energy of $A_{M \times N}$ can be mathematically expressed as

$$\mathrm{E_I} = \sum_{i=1}^{\mathrm{N}} \beta_{\mathrm{i}}^2 \tag{7}$$

The singular values of the S matrix are in descending order such that

$$\beta_1^2 \ge \beta_2^2 \ge \beta_3^2 \ge \ldots \beta_{\mathrm{N}}^2 \tag{8}$$

and the term $u_i\beta_i v_i$ with small values of i contain most of the information. Therefore, truncating the β value to an optimum number helps reducing the size of the data.

In this research, the DCT-II of the $MECG_{r\times 8}$ matrix is computed, and the resulting DCT coefficient-matrix is denoted as $MDCT_{r\times 8}$. Fig. 2 shows an exemplary content of $MECG_{r\times 8}$ and its corresponding $MDCT_{r\times 8}$. In Fig. 2A, the shown MECG signal (File #s0224_rem) is taken from PTB Diagnostic ECG database (ptbdb), and only the first five seconds of MECG, i.e., 1250 samples of each of the ECG leads are shown for better visualization. However, all the coefficients of the *MDCT* matrix are shown in Fig. 2B. From Fig. 2B it can be seen that the amplitudes of a few hundred DCT coefficients at the end of each of the eight columns of the *MDCT* matrix are much lower compared to the corresponding leading coefficients. This observation leads us to explore the optimum number of the DCT coefficients that needs to faithfully reconstruct the MECG signals.

Now, only a certain percent (which is denoted as α) of the total number rows of all the eight columns of the $MDCT_{r\times 8}$ matrix is taken for processing and kept in another matrix $Temp_{\lambda\times 8}$, where $\lambda = (\alpha\,\%\ of\ r)$. Next, SVD of $Temp_{\lambda\times 8}$ is computed.

$$\mathrm{Temp}_{\lambda\times 8} = \mathrm{U}_{\lambda\times\lambda}\,\mathrm{S}_{\lambda\times 8}\,\mathrm{V}^{\mathrm{T}}_{8\times 8} \tag{9}$$

Then, the reverse-SVD operation is computed to approximate $Temp_{\lambda\times 8}$ matrix with an optimum number of β values. First, $Temp_{\lambda\times 8}$ matrix is approximated with β_1 only, which is denoted as $\overline{Temp_{\lambda\times 8}|\beta_1}$. Next, the inverse-DCT operation is performed on $\overline{Temp_{\lambda\times 8}|\beta_1}$ after zero-padding for the rest of the rows $(r-\lambda)$ to approximate $MECG_{r\times 8}$. The inverse-DCT-approximated matrix is denoted as $\overline{MECG_{r\times 8}}$. From $\overline{MECG_{r\times 8}}$, the eight ECG leads are reconstructed through proper up-sampling and amplitude de-normalization operations. Next, the error between each pair of the original and reconstructed ECG leads is calculated. The technique which is used to measure the error between the original and reconstructed ECG leads is described later in this Section. If the error in *any* of the eight reconstructed ECG leads exceeds the user-defined value of the error-threshold (Th_{UD}), then the reverse-SVD operation is again computed taking two singular values, i.e., β_1 and β_2, and the eight ECG leads are again reconstructed through inverse-DCT, up-sampling and amplitude de-normalization operations. If it is found that the desired error criteria is even not satisfied while reconstructing MECG signals using all the eight singular values with α% of the number of rows of the $MDCT_{r\times 8}$ matrix, then α is incremented by an amount γ, i.e., $\alpha\leftarrow\alpha+\gamma$, and the same operation is iterated. The optimum values of α and β for which the user-defined MECG reconstruction-error criteria is satisfied, are denoted as α_{opt} and β_{opt}, respectively. The algorithm of calculation of α_{opt} and β_{opt} is given below.

$MDCT_{r\times 8} \leftarrow DCT2(MECG_{r\times 8})$
$\alpha \leftarrow$ initial value
$\lambda \leftarrow 0.01 \times \alpha \times r$
while $\alpha \le 100$
  $Temp_{\lambda\times 8} \leftarrow MDCT_{(1:\lambda)\times 8}$
  $U_{\lambda\times\lambda}\,S_{\lambda\times 8}\,V^{T}_{8\times 8} \leftarrow SVD\left(Temp_{\lambda\times 8}\right)$
  for $i = 1:8$
    $\overline{Temp_{\lambda\times 8}} \leftarrow U_{\lambda\times i}\,S_{i\times i}\,V^{T}_{8\times i}$
    $Z \leftarrow zeros(r, 8)$
    $Z(1:\lambda, :) \leftarrow \overline{Temp_{\lambda\times 8}}$
    $\overline{MECG_{r\times 8}} \leftarrow iDCT2(Z)$

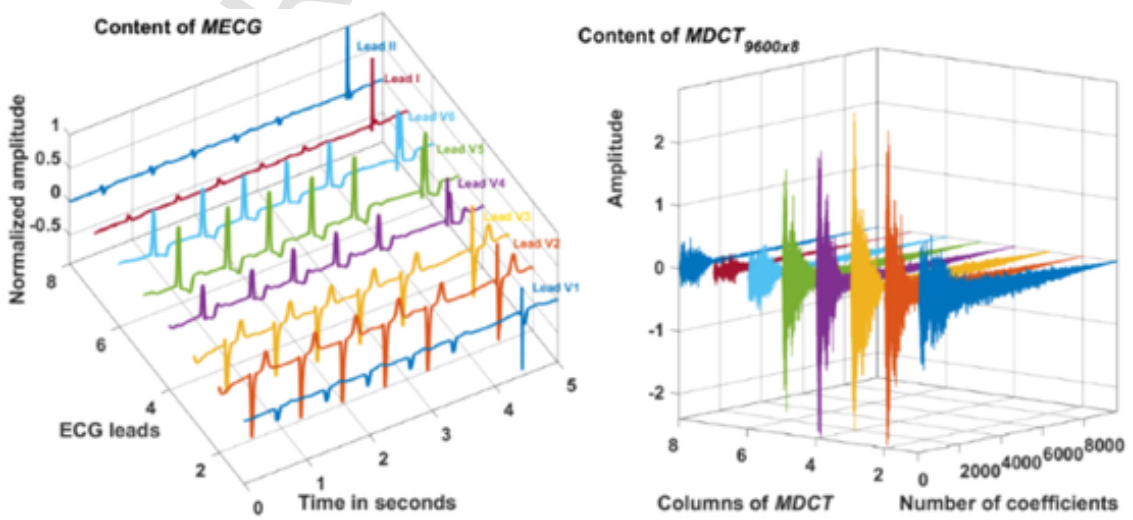

Fig. 2. (A) Preprocessed MECG signal of duration five seconds only; File #s0224_rem, ptbdb, (B) corresponding *MDCT*.

```
        flag ← 0
        for j ← 1: 8
            reconstructed ECG lead(j) ← up-sampling, amplitude de-normalization (MECG_{r×j})
          E(j) ← error(original ECG lead(j), reconstructed ECG lead(j) )
          if E(j) > Th_UD
            flag ← 1
            break
          end
        end
        if flag = =0
          α_opt ← λ
          β_opt ← i
          [ME_P, L_P] ← max (E)
          break
        end
    end
    if flag = =0
        break
    else
        α ← α+γ
    end
    end
```

ME_P is the predicted maximum ECG reconstruction error, and L_P is the corresponding ECG lead. In all other 7 ECG leads the reconstruction error would be less than ME_P. In this proposed algorithm, initially, 10% of the total number of rows of the $MDCT_{r \times 8}$ matrix is taken for computing the SVD, i.e., α is initially set to 10%, and incremented by 10% (i.e., γ = 10%). SVD of $MDCT_{r \times 8}$ matrix results in U, S, and V^T metrics of dimensions, respectively, ($r \times r$), ($r \times 8$), and (8×8). However, the algorithm described above for calculating α_{opt} and β_{opt} reduces the dimension of the S matrix from ($r \times 8$) to ($\beta_{opt} \times \beta_{opt}$), and consequently the dimensions of the U and V^T metrics reduces from ($r \times r$) to ($\alpha_{opt} \times \beta_{opt}$) and ($8 \times 8$) to ($8 \times \beta_{opt}$), respectively. The above-described technique using DCT and SVD operations together help reducing the number of rows and columns to be processed further. The amount of reduction in terms of the number of samples in the $MECG_{r \times 8}$ matrix that could be obtained only through optimally truncating the DCT coefficients and singular values can be expressed as below.

$$\mathrm{R}\left(\alpha_{\mathrm{opt}}, \beta_{\mathrm{opt}}\right) = \frac{r \times 8}{\left(\alpha_{\mathrm{opt}} \times \beta_{\mathrm{opt}}\right) + \beta_{\mathrm{opt}} + \left(8 \times \beta_{\mathrm{opt}}\right)} \tag{10}$$

where $R(\alpha_{opt},\beta_{opt})$ is the data-reduction ratio, and r is the number of samples in each of the eight MECG leads after down-sampling. The lower the values of both α_{opt} and β_{opt} the higher the data-reduction ratio, i.e., the compression performance. Intuitionally, (i) the higher the intra sample correlation, the lower the value of α_{opt}, and (ii) the higher the inter-lead correlation, the lower the value of β_{opt}.

Now, the coefficients of the $U_{\alpha_{opt} \times \beta_{opt}}$ matrix are compressed in a *strict lossless* manner, the coefficients of the $V^T{}_{8 \times \beta_{opt}}$ matrix are compressed using a *near-lossless* technique, and β_{opt} singular values are stored unaltered. Therefore, most of the MECG signal reconstruction error arises from the truncation of the DCT coefficients and singular values and up-sampling and down-sampling operations. As described above, the aggregated contribution of these operations to the MECG signal reconstruction error can be estimated in advance, which enables to (i) control the quality of the reconstructed MECG signals precisely, and (ii) predict the lead-wise reconstruction-performance from the values of ME_P and L_P.

Wavelet energy-based diagnostic distortion (WEDD) is a technique [31] for assessing the quality of a reconstructed ECG signal. This technique is used in this research work in order to measure the error between each pair of the eight original and reconstructed ECG leads. The WEDD technique decomposes both the original and reconstructed ECG signals into $L + 1$ number of frequency bands (L number of detail-coefficient bands, and one approximation-coefficient band) using wavelet transform. The dynamic weight of each of these $L + 1$ frequency bands of the original ECG signal is calculated from as follows.

$$\mathrm{w_l} = \frac{\sum_{i=1}^{\mathrm{n}} \mathrm{D_l^2\,(i)}}{\sum_{j=1}^{L+1} \sum_{i=1}^{\mathrm{n}} \mathrm{D_j^2\,(i)}} \tag{11}$$

$$l = 1,\ 2, \ldots,\ L+1$$

where w_l is the dynamic weight of the l^{th} wavelet frequency band, n denotes the number of coefficients in the l^{th} frequency band, and $D_l(i)$ is the i^{th} coefficient in the l^{th} frequency band of the original ECG signal. The error between the original and reconstructed ECG signals' wavelet coefficients in then calculated as below.

$$\mathrm{WPRD_l} = \sqrt{\frac{\sum_{i=1}^{n}\left(\mathrm{D_l(i)} - \overline{\mathrm{D_l(i)}}\right)^2}{\sum_{i=1}^{n}\mathrm{D_l^2(i)}}} \quad (12)$$

$l = 1,\ 2, \ldots,\ L+1$

where $WPRD_l$ is the error between the original and reconstructed ECG signal-coefficients in the l^{th} frequency band, and $\overline{D_l(i)}\Big)$ is the i^{th} coefficient in the l^{th} frequency band of the reconstructed ECG signal. And finally, the WEDD is calculated as follows.

$$\mathrm{WEDD\,(\%)} = \left(\sum_{l=1}^{L+1} \mathrm{w_l} \times \mathrm{WPRD_l}\right) \times\ 100 \quad (13)$$

In this research work, '*bior6.8*' wavelet filter is used to decompose each of the eight original and reconstructed ECG leads into $L + 1$ number of frequency bands ($L = \lfloor log_2(sampling\ frequency) - 2.96 \rfloor$) [31]. As per the WEDD criteria [31], the quality of a reconstructed ECG signal is considered as: (1) 'excellent', if the WEDD value is less than 4.517%, (2) 'very good', if it is within the range 4.517%–6.914%, (3) 'good', if it is within the range 6.914%–11.125%, (4) 'not bad', if it is within the range 11.125%–13.56%, and (5) 'bad', if it is >13.56%. The values of α_{opt} and β_{opt} are calculated based on a user-defined threshold value (Th_{UD}) of WEDD.

3.3. Steganography and LL-ACE of the left singular matrix coefficient

The ASCII values of patients' confidential information (first and last names, date of birth, gender, systolic and diastolic blood pressures, weight, body temperature, postal and email addresses, phone number) are initially stored in an array with '*space*' delimiters (the ASCII value of '*space*' is 32) among the entities. Now, the array is arranged in the form of a matrix, which is denoted as *PCI* (patient's confidential information), of dimension $n \times \beta_{opt}$. The value of n varies with the total number of ASCII values in the array. The coefficients of the $U_{\alpha_{opt}\times\beta_{opt}}$ matrix are always in the floating-point format and are computed up to three decimal places of accuracy, whereas the ASCII values are of integer data type and vary from 0 to 255. To bring the coefficients of $U_{\alpha_{opt}\times\beta_{opt}}$ and $PCI_{n\times\beta_{opt}}$ matrices to the same magnitude scale, the $U_{\alpha_{opt}\times\beta_{opt}}$ matrix coefficients are amplified by a factor of 1000. Now, the amplified $U_{\alpha_{opt}\times\beta_{opt}}$ matrix coefficients are concatenated with the $PCI_{n\times\beta_{opt}}$ matrix. The concatenated matrix of dimension (α_{opt} + n) × β_{opt} is denoted as $\widetilde{U}$. Now, the coefficients of the $\widetilde{U}$ matrix are compressed using a LL-ACE-based compression algorithm. The LL-ACE, proposed in [32], is a low-complex yet high performance lossless biosignal compression algorithm. The LL-ACE technique [32] is used in this research work with one modification.

The first-difference of the $\widetilde{U}$ matrix coefficients is computed. The LL-ACE technique proposed in [32], clips any non-ASCII value (i.e., >255) to 255, which introduces unwanted glitches in the reconstructed signal. To overcome this, in this research, it is checked in first-difference data so as to find any value that is greater than 255. If any data value is found to be greater than 255, it is replaced with 255, and the corresponding data-value and its index are stored in a file named 'ASCIIdiff.dat'. These indices are used to restore back the original values in the first-difference data at the time of reconstruction.

The LL-ACE algorithm processes a group of eight coefficients at a time. Now, the first eight coefficients are taken from the first difference data. The sign-byte of these eight coefficients is generated. The positive and negative coefficients are marked by a binary 0 and 1, respectively. Now, the decimal-equivalent of these eight bits is calculated (which is considered as the sign-byte). Next, all these eight coefficients are made positive following sign-byte generation. The following example illustrates the process of sign-byte generation.

First-difference	12	2	6	3	−8	−10	−5	−7
Sign-bits	0	0	0	0	1	1	1	1
Sign-byte	15							
ASCII character	☼							
Make positive	12	2	6	3	8	10	5	7

After the sign-byte generation operation, the neighboring coefficients are grouped using various merging techniques to reduce the size of the data. These merging techniques are reversible, and hence the merged-coefficients can be separated properly at the time of reconstruction. The merging techniques are discussed below.

Technique #1: If all these eight coefficients are found to be identical, they are represented by a single integer.

Technique #2: If *Technique #1* is not applicable on these eight coefficients, i.e., they are not found identical, then *Technique #2* is applied. In *Technique #*2 it is checked as to whether two neighbor coefficients are single-digited (≤9) or not. If both the neighbor coefficients are found to be single-digited, then the 1st coefficient is multiplied by 10 and added to the 2nd coefficient. Therefore, two neighbor coefficients are grouped into a single integer. The following example illustrates *Technique #2*.

Coefficients	1	4	0	5	1	5	0	1
Technique #2	14		5		15		1	
ASCII character	♫		♣		☼		☺	

Technique #3: If it is found that all the eight coefficients are grouped into four using *Technique #2*, and if it is again found that each of these four grouped coefficients are ≤ 15, then they are regrouped in their binary domain. Each of those grouped-coefficient is converted to their four bit binary equivalent. Now, two neighboring nibbles (1 nibble $=$ 4 bits) are concatenated to form an eight bit binary string, and finally the string is converted into its decimal equivalent. The following example illustrates *Technique #3*.

Coefficients		1	4	0	5	1	5	0	1
Technique #2		14		5		15		1	
Technique #3	Nibble	1110		0101		1111		0001	
	String	11,100,101				11,110,001			
	Decimal	229				241			
ASCII character		σ				±			

Technique #4: If it is found that *Technique #2* is only partly applicable to the eight coefficients, then those pairs of coefficients on which *Technique #2* is not applicable, are kept unaltered. An extra byte (say *X[]*) is used to denote the indices of these unaltered pairs. The following example illustrates this point.

Coefficients	1	2	0	3	12	4	5	18
Reduced data	12		3		12	4	5	18
ASCII character	♀		♥		♀	♦	♣	↕
X	0		0		1	1	1	1
	X[1]		*X[2]*		*X[3]*	*X[4]*	*X[5]*	*X[6]*
Decimal equivalent of *X*	15							
ASCII character of *X*	☼							

These grouped, non-grouped integers along with other necessary information such as sign-byte, the decimal equivalent of *X[]* are printed in an output file named 'CECG.dat' in the form of their corresponding ASCII characters. The LL-ACE technique is applied iteratively taking eight consecutive samples at a time until all the coefficients of the first-difference of the $\widetilde{U}$ matrix are compressed. Each set of characters is separated from the next set by using an '*Enter*' character. The original *U*-matrix coefficients are floating-point numbers, and as per the IEEE 754 Standard, a floating-point number occupies four bytes of computer memory. Therefore, eight *U*-matrix coefficients need 32-bytes of memory to store. On the other hand, an ASCII character takes only 1-byte of computer memory. The LL-ACE technique tries to represent eight floating-point numbers with a fewer number of ASCII characters and thus achieving a data-compression. *Technique #1* yields a compression ratio of 16 ($= \frac{8 \times 4bytes}{one\ sign\ byte + one\ ASCII\ character}$). Likewise, *Technique #2* yields a compression ratio of 6.4, *Technique #3* yields a compression ratio of 10.67, and *Technique #4* yields a range of compression ratio ranging from 3.2 to 4.57. Fig. 3 shows an example of the content of the $\widetilde{U}$ matrix coefficients and its compressed version. From this Figure it can be seen that alongside compression, the LL-ACE technique transforms the coefficients in such a domain where the patients' information becomes disguised.

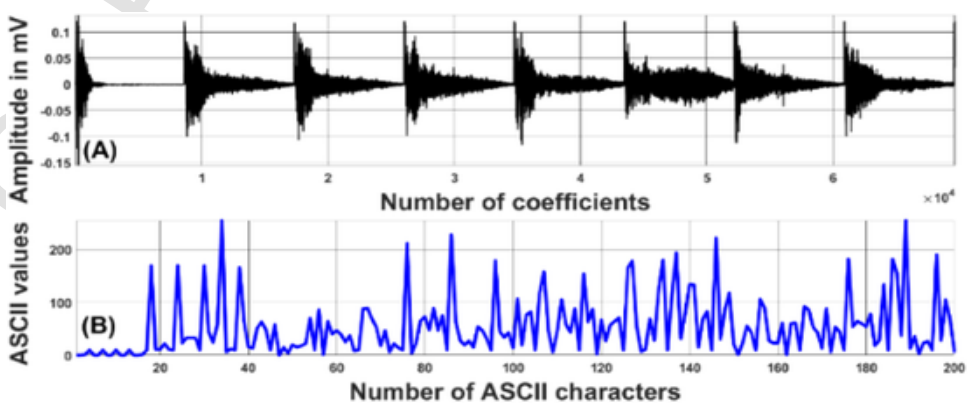

Fig. 3. (A) The $\widetilde{U}$ matrix coefficients, and (B) compressed $\widetilde{U}$ matrix coefficients.

3.4. Quantization of the right singular matrix coefficient

The coefficients of the right singular matrix ($V^T_{8\times\beta_{opt}}$) are quantized using a uniform quantizer of 2^{16} levels. The quantized values are encoded using 16-bits. Now, each of the 16-bit data stream is divided into two separate bytes. Each byte is converted into its corresponding ASCII character. The ASCII characters are written to an output file named 'Vcoeff.dat'. Since the V^T matrix coefficients are encoded using 16-bits, the contribution of the quantization error to the signal to noise ratio (SNR_{dB}) is 98.081dB. The contribution of the $V^T_{8\times\beta_{opt}}$ matrix quantization error to the MECG signal reconstruction is very small, and hence, it is not considered while estimating α_{opt} and β_{opt} in Section 3.2.

3.5. Generation of the security-key

A few crucial information, whose ranges are very wide and dynamic, have been selected to use as the security-key so as to safeguard the compressed MECG data as well as the patient's confidential information from intruders' attack. The entities that we have chosen to use in this research as the security-key are (1) the down-sampling factor *D*, (2) *r* (3) $ANF_{1\times 8}$ (4) α_{opt}, (5) the number of rows *n* in the *PCI* matrix, (6) maximum and minimum values of the $V^T_{8\times\beta_{opt}}$ matrix coefficients, and (7) β_{opt} singular values. These entities are saved in a file named 'SecKey.dat'. The value of *D* depends on the sampling frequency of the original MECG signal, and it is seen in this research work that it varies between 250 Hz, 500 Hz and 1 kHz across different MECG databases. The value of *r* depends on the length of the MECG signal and *D*. The values of the amplitude normalization factor ($ANF_{1\times 8}$) depends on the gain value of the MECG acquisition unit, and its range could be a few mV to hundreds of mV. In this research, it is experimentally observed that each of the eight amplitude normalization factors varies from −6000 to 6000 across different MECG databases. The value of α_{opt} can have a dynamic range, and it depends on the (1) intra and inter sample correlation among the MECG leads, and (2) the number of rows of the $MDCT_{r\times 8}$ matrix. The number of rows (*n*) in the patient information matrix *PCI* depends on the number ASCII characters in the patient information data and the value of β_{opt}. In this present research work, it has been experimentally observed that both the maximum and minimum values of the $V^T_{8\times\beta_{opt}}$ matrix-coefficients vary from −0.999 mV to 0.999 mV. The number of singular values (β_{opt}) could vary from one to eight, and the magnitude of each of these eight singular values has been experimentally observed to vary between 0 and 100. Since the range of most of these entities are unknown, it is also not possible for us to accurately calculate the strength of the security-key. However, the probability of guesstimating only the maximum and minimum values of the $V^T_{8\times\beta_{opt}}$ matrix-coefficients and *D* is: $\left(\frac{1}{1999}\times\frac{1}{1999}\times\frac{1}{3}\right) = 8.3417\times10^{-8}$, which is very close to 0. This suggests that even a brute-force attack, which checks with all the possible combinations of all the entities of the keys to break the security, needs $1999\times1999\times3 = 11988003$ attempts to guesstimate these *three* entities only out of seven.

4. MECG reconstruction and patient's information extraction

The compressed steganographed-MECG data is stored in four files (1) ASCIIdiff.dat, (2) CECG.dat, (3) Vcoeff.dat and (4) SecKey.dat. The contents of all these files are needed to faithfully reconstruct the MECG signals and restore patients' confidential information. All the information is fetched from these four files and are stored temporarily in the computer memory. First, the β_{opt} values are arranged to reform the diagonal $S_{\beta_{opt}\times\beta_{opt}}$ matrix.

Next, the $V^T_{8\times\beta_{opt}}$ matrix is regenerated using a reverse approach of the technique that is used in Section 3.4 for compression. The ASCII characters are fetched from the 'Vcoeff.dat' file. Each of these ASCII characters are mapped to their corresponding ASCII values. Each of these ASCII values are then converted to an eight-bit binary equivalent, and two neighboring eight-bit binary numbers are concatenated to form a 16-bit binary string. Now, using the maximum and minimum values of the $V^T_{8\times\beta_{opt}}$ matrix coefficients each of the 16-bit binary strings is decoded to regenerate the coefficients. These coefficients are then arranged to reform the $V^T_{8\times\beta_{opt}}$ matrix.

Now, the $\widetilde{U}_{(\alpha_{opt}+n)\times\beta_{opt}}$ matrix coefficients are decoded using a technique, which is reverse of the approach implemented in Section 3.3. First, the ASCII characters (which are fetched from the file 'CECG.dat') are converted to their corresponding ASCII values. One set of ASCII values is taken at-a-time for decoding. If one set of ASCII values contains only one integer (except the sign-byte), it signifies that *Technique #1* was applied at the time of LL-ACE, and the corresponding eight coefficients are regenerated easily. If one set of ASCII values contains four integers (except the sign-byte), it signifies that *Technique #2* was applied at the time of LL-ACE. These four integers are ungrouped into eight by dividing each of these integers by 10 and then separating out the quotients and reminders. If a set of ASCII values contains two integers (except the sign-byte), it signifies that *Technique #3* was applied at the time of LL-ACE. These two integers are converted to their corresponding eight-bit binary equivalent. Each of these two eight bits binary numbers is separated into two nibbles and thus generating four nibbles in total. These four nibbles are then converted to their corresponding decimal equivalent. These four decimal values are ungrouped to eight coefficients by using a reverse programming approach of *Technique #2*. If one set of ASCII values contains more than four integers (except the sign-byte), it signifies that *Technique #4* was applied at the time of LL-ACE, and a reverse programming approach of *Technique #4* is used to ungroup these integers with the help of the extra byte *X[]*. This is illustrated by considering the following example, which is the reverse of the one considered in Section 3.3.

ASCII character of *X[]*	☼							
Decimal equivalent of *X[]*	15							
Binary equivalent of *X[]*	0		0		1	1	1	1
ASCII character	♀		♥		♀	♦	♣	↕
ASCII values	12		3		12	4	5	18
Divide by 10 Q→quotient, R→reminder	Q:1, R:2		Q:0, R:3					
Coefficients	1	2	0	3	12	4	5	18

The presence of binary '0' and '1' in *X[]* indicate a grouped and non-grouped ASCII value, respectively. Next, the sign-byte is converted into its corresponding eight-bit binary equivalent. In the binary string, if any bit is found to be '1', then the corresponding positional un-grouped integer is multiplied by −1. The process of un-grouping is iterated until all sets of the ASCII values are ungrouped. These ungrouped data are the first-difference of the $\widetilde{U}$ matrix coefficients. Now, the content of the 'ASCIIdiff.dat' file is fetched. This file contains the indices and the actual positional contents of those indices in the first-difference data-stream. The contents of the corresponding indices of the ungrouped data are replaced accordingly. Next, the reverse operation of the first-difference is performed on those ungrouped data, and are arranged to reform the $\widetilde{U}$ matrix of dimension $(\alpha_{opt} + n) \times \beta_{opt}$. The values of α_{opt}, n, and β_{opt} are fetched from the file 'SecKey.dat'. The $\widetilde{U}$ matrix is then separated into $U_{\alpha_{opt}\times\beta_{opt}}$ and $PCI_{n\times\beta_{opt}}$matrices. The patient's confidential information is restored from the ASCII values of the *PCI* matrix. All the coefficients of the *U* matrix are divided by 1000, as the reverse was performed during compression.

Now, the$U_{\alpha_{opt}\times\beta_{opt}}$, $S_{\beta_{opt}\times\beta_{opt}}$, and $V^T_{8\times\beta_{opt}}$ matrices are multiplied, i.e., the reverse-SVD operation is performed to approximate the $MDCT_{\alpha_{opt}\times 8}$ matrix, which is denoted as $\overline{MDCT_{\alpha_{opt}\times 8}}$. Next, the inverse-DCT operation is performed on the $\overline{MDCT_{\alpha_{opt}\times 8}}$ matrix after zero-padding with $(r - \alpha_{opt})$ number of rows and eight columns to approximate the $MECG_{r\times 8}$ matrix, which is denoted as $\overline{MECG_{r\times 8}}$. Finally, the eight ECG leads are reconstructed from the $\overline{MECG_{r\times 8}}$ matrix through up-sampling and amplitude-denormalization utilizing the values of D and $ANF_{1\times 8}$, respectively. Fig. 4 shows and example of the original, reconstructed and the reconstruction-errors of the $\widetilde{U}$ and V^T matrix-coefficients. From this figure it can be seen that the reconstruction errors of the $\widetilde{U}$ matrix coefficients are zero, and the reconstruction errors of the V^T matrix coefficients are also very low (of the order of 10^{-4}).

5. Results

Clinical evaluation by experienced clinicians remains the most reliable method when it comes to validating the clinical quality of the reconstructed biosignals. However, several clinically accepted numerical methods also exist for assessing the degree of preservation of clinical morphology in the reconstructed ECG signals. In this study, the quality of the reconstructed MECG signals is assessed using both quantitative and qualitative measures. The quantitative measures, which is used in this work is WEDD. Semi-blind mean opinion score (MOS) test [33] has been carried out to evaluate the performance of the proposed *QSMECGcomp* algorithm qualitatively. The compression ratio (CR), a standard performance metric for compression algorithms, is defined as

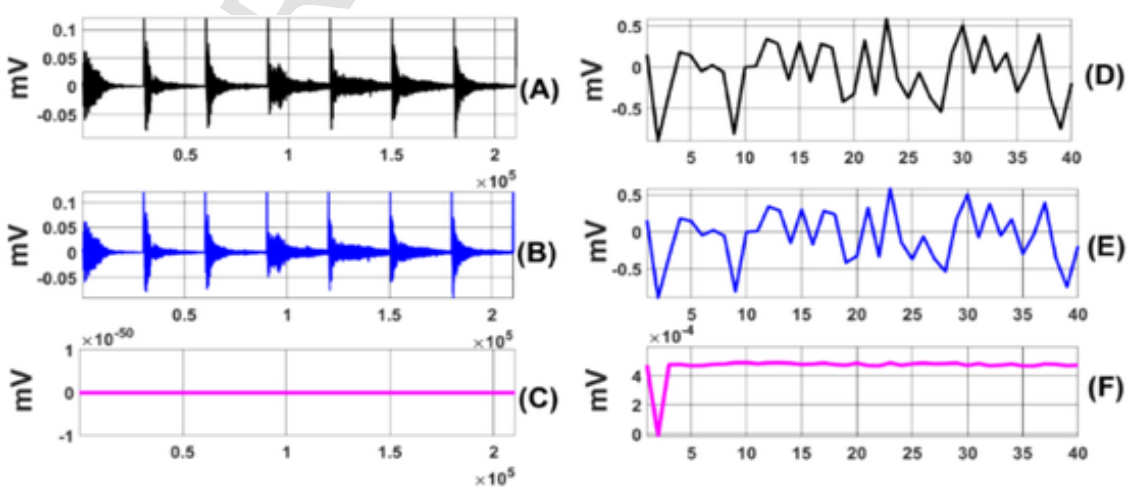

Fig. 4. (A) original $\widetilde{U}$ matrix coefficients, (B) reconstructed $\widetilde{U}$ matrix coefficients, (C) Error between the coefficients shown in (A) and (B), (D) original *V* matrix coefficients, (E) reconstructed *V* matrix coefficients, (F) Error between the coefficients shown in (D) and (E). The x-axes of all the subplots represent the number of samples.

$$CR = \frac{S_O}{S_C} \tag{14}$$

where S_O is the size of the original data, and S_C is the size of the compressed data. In this research, S_O refers to the combined size of the files 'Original ECG.dat' and patient's information, and S_C refers to the cumulative size of the four files ASCIIdiff.dat, CECG.dat, Vcoeff.dat and SecKey.dat. Lower values of WEDD and MOS, and higher values of CR, indicate better performance. MECG signals collected from three publicly available online ECG databases serve as evaluation testbeds for the proposed *QSMECGcomp* algorithm. The details of the collected MECG signals from these databases are given in Table 2. Lead-wise WEDD is calculated upon reconstruction of the MECG signals, and the (i) maximum error (ME_R), and (ii) corresponding lead (L_R) is identified. The difference between the predicted-maximum and the actual-maximum reconstruction errors is defined as

$$\mathrm{WEDD_{diff}}\,(\%) = \mathrm{ME_R}\,(\%) - \mathrm{ME_P}\,(\%) \tag{15}$$

The value of $WEDD_{diff}$ could be positive or negative. A negative value of $WEDD_{diff}$ indicates good quality control. However, the value of ME_R should not exceed the value of Th_{UD}. The performance of the proposed *QSMECGcomp* algorithm is tested on all MECG signals from these three databases, using varying sizes of patient information for a Th_{UD} value of 6.914%, and the results are presented in Table 3. According to the WEDD criteria a Th_{UD} value of 6.914% indicates a 'very good' quality of ECG reconstruction. From this Table it can be noted that (i) although minimal, the average CR decreases with increasing the size of the patient information data, but (ii) the size of the patient information data is not correlated with the quality of MECG reconstruction anyway, and (iii) the average value of $WEDD_{diff}$ value is very low across all three databases and is negative for the MECG signals from PTBDB, indicating excellent quality control of the proposed algorithm.

In this research work, the maximum and minimum CR values obtained using the *QSMECGcomp* algorithm on PTBDB are 738.9 for the file number s0448 and 32.85 for the file number s0224 with ME_R values of 4.68% and 4.92%, respectively. Fig. 5 shows the histogram of the CR and $WEDD_{diff}$ values for all the MECG signals from the PTBDB, SNHDB and INCART databases, evaluated at different patient-information sizes with Th_{UD} = 6.914%. Figs. 6 and 7 show the original MECG signals, reconstructed MECG signals and the corresponding reconstruction errors of these two PTBDB ECG signals. Comparing Figs. 6 and 7, it can be intuitionally concluded that the correlation among the ECG leads of the file s0448 is much higher than that in file s0224. The changes in amplitudes and polarity among the leads in file s0448 occur more consistently than those in file s0224, which in turn, helps the *QSMECGcomp* algorithm use smaller α_{opt} and β_{opt} values for the MECG signals of file s0448 than for file s0224. It has been observed that for MECG data from these three databases the L_P and L_R always match, providing further evidence of good quality control.

Alongside the quantitative measures, qualitative (i.e., subjective) measures are also equally important for assessing the true quality of the reconstructed MECG signals. The Mean Opinion Score (MOS) test is a subjective quality assessment method in which the quality of an output signal (such as a 1D signal, image, audio, or video) is evaluated by the domain experts. There are two types of MOS tests: (1) Blind MOS test: the evaluators are not informed whether the signal they are rating is original, compressed, processed, reconstructed, or distorted, and (2) Semi-blind MOS test: the evaluators are provided with both the original and the reconstructed sig-

Table 2
The details of the collected MECG signals.

Databases and Sampling rate	No. of records	ECG duration/lead	Types
PTB Diagnostic ECG database (ptbdb) [34], 1000Hz	549	32 s to 120s	Normal and 8 different types of abnormalities
Shaoxing and Ningbo Hospital ECG Database (SNHDB) [36], 500Hz	45,152	10s	Normal and arrhythmias
St Petersburg INCART 12-lead Arrhythmia database [34], 250Hz	75	30 min	10 different types of abnormalities
Total	**7.46** days/lead		

Table 3
Performance of the *QSMECGcomp* algorithm for Th_{UD} = 6.914%.

Database	PI (bytes)	Mean ME_P	Mean ME_R	Mean $WEDD_{diff}$ ±SD	Mean CR
PTBDB	125	5.91	5.89	−0.02 ± 0.09	148.16
	250	5.91	5.89	−0.02 ± 0.09	147.03
	375	5.91	5.89	−0.02 ± 0.09	145.83
	500	5.91	5.89	−0.02 ± 0.09	145.28
SNHDB	125	5.03	4.90	0.17 ± 0.08	46.87
	250	5.03	4.90	0.17 ± 0.08	46.41
	375	5.03	4.90	0.17 ± 0.08	46.28
	500	5.03	4.90	0.17 ± 0.08	45.97
INCART	125	6.04	6.05	0.002 ± 0.006	27.65
	250	6.04	6.05	0.002 ± 0.006	27.61
	375	6.04	6.05	0.002 ± 0.006	27.37
	500	6.04	6.05	0.002 ± 0.006	27.12

PI→patient's information.

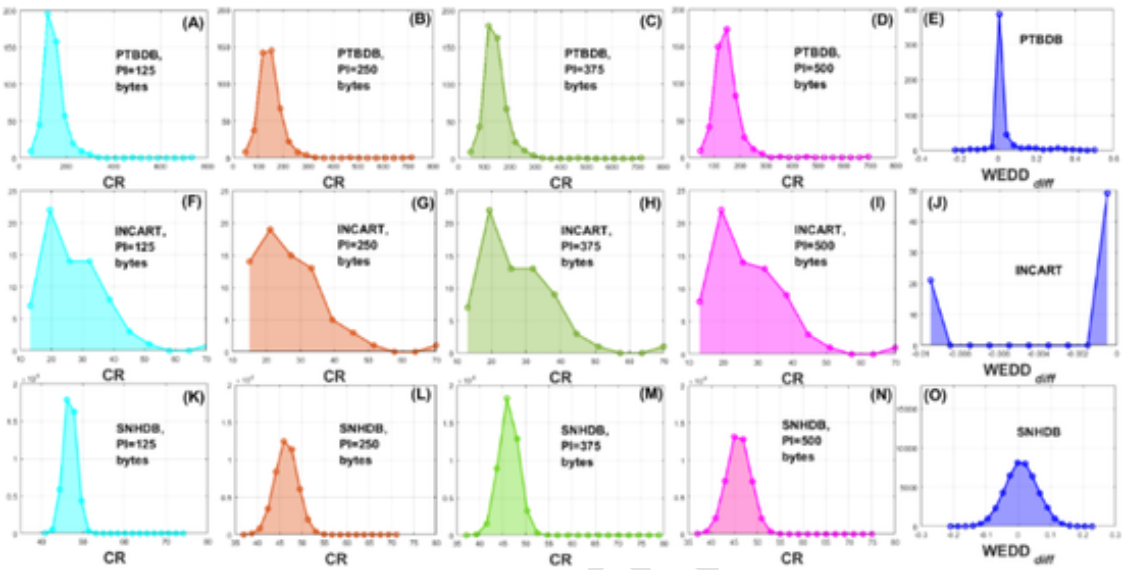

Fig. 5. Histogram plot of the CR and $WEDD_{diff}$ values for all the MECG signals of PTBDB, SNHDB and INCART databases for different sizes of patient-information for Th_{UD} = 6.914%. Y-axes of all the subfigures represent the number of occurrences. (A) histogram of CR, PI = 125bytes, PTBDB, (B) histogram of CR, PI = 250bytes, PTBDB, (C) histogram of CR, PI = 375bytes, PTBDB, (D) histogram of CR, PI = 500bytes, PTBDB, (E) histogram of $WEDD_{diff}$, PTBDB, (F) histogram of CR, PI = 125bytes, INCART, (G) histogram of CR, PI = 250bytes, INCART, (H) histogram of CR, PI = 375bytes, INCART, (I) histogram of CR, PI = 500bytes, INCART, (J) histogram of $WEDD_{diff}$, INCART, (K) histogram of CR, PI = 125bytes, SNHDB, (L) histogram of CR, PI = 250bytes, SNHDB, (M) histogram of CR, PI = 375bytes, SNHDB, (N) histogram of CR, PI = 500bytes, SNHDB, (O) histogram of $WEDD_{diff}$, SNHDB.

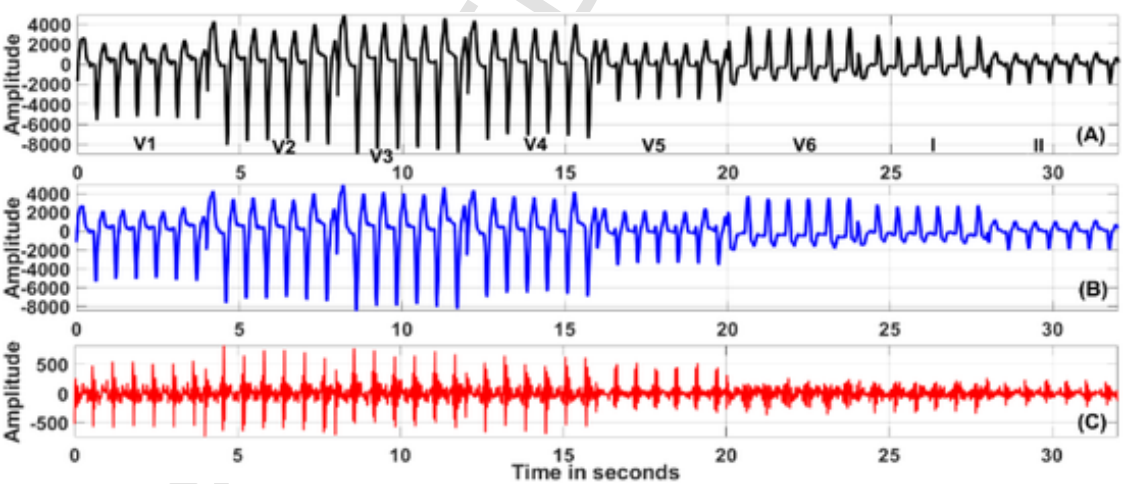

Fig. 6. (A) Original MECG signals of File# s0448 (four seconds of each lead), (B) reconstructed MECG signals (CR = 738.9, ME_R = 4.68%, $L_P = L_R$), and (C) error between the signals shown in (A) and (B).

nals and are aware of which one is which [38]. In this case, they are asked to assess whether the clinical morphology has been compromised in the reconstructed signal - for example, whether a diagnosis based only on the reconstructed signal would differ from that based on the original. A semi-blind MOS test [33] was conducted with seven evaluators (academicians with strong backgrounds in digital signal, bio-image, and bio-signal processing) has been carried out. Twelve ECG features (including amplitude, shape, and duration of the QRS complex; amplitudes, polarities, and durations of the T and P waves; elevation of the ST segment; and PR and QT intervals) were considered for the MOS test. Original and reconstructed MECG signals chosen from these two databases were provided to the evaluators, and they were asked to compare these twelve features of the reconstructed MECG signals with their original counterparts and assign a score based on the level of resemblance using the following scale: 5 for exact replication, 4 for very good, 3 for good, 2 for not bad, and 1 for very bad. Results are shown in Table 3. The MOS value of a particular ECG feature F in the reconstructed MECG signal is evaluated using

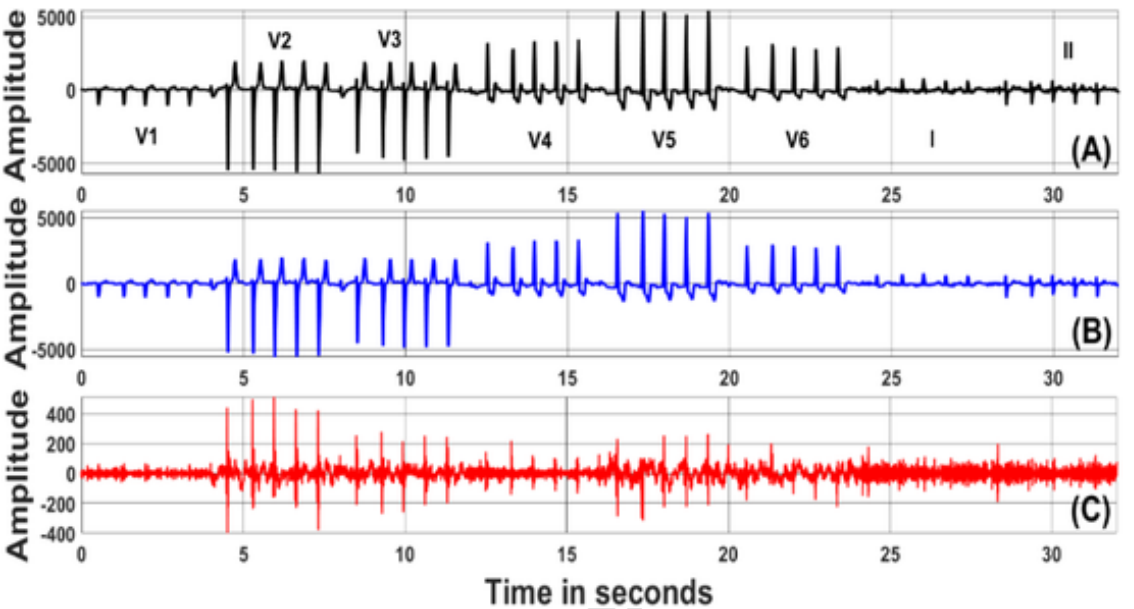

Fig. 7. (A) Original MECG signals of File# s0224 (four seconds of each lead), (B) reconstructed MECG signals (CR = 32.85, $ME_R = 4.92\%$, $L_P = L_R$), and (C) error between the signals shown in (A) and (B).

$$\mathrm{MOS\,(F)} = \frac{1}{\mathrm{N_{EV}}} \sum_{\mathrm{EV}=1}^{\mathrm{N_{EV}}} \mathrm{Q\,(EV, F)} \tag{16}$$

where N_{EV} is the total number of evaluators and Q is the quality rating of the F^{th} MECG feature given by the EV^{th} evaluator. MOS of the reconstructed MECG signal is calculated using the equation

$$\mathrm{MOS} = \frac{1}{\mathrm{N_{EV}N_F}} \sum_{\mathrm{EV}=1}^{\mathrm{N_{EV}}} \sum_{F=1}^{\mathrm{N_F}} \mathrm{Q\,(EV, F)} \tag{17}$$

where N_F is the total number of features that are considered, which is 12 in this study. Finally, the gold standard MOS error of each of the ECG features and the overall reconstructed MECG signal are calculated using Eqs. (18) and (19), respectively. From Table 4, it can be seen that as per the gold-standard MOS error criteria described in [33], each of the features as well as the reconstructed MECG signal fall under the category 'very good'.

$$\mathrm{MOS_{Fe}} = \left(1 - \frac{\mathrm{MOS\,(F)}}{5}\right) \times 100\% \tag{18}$$

$$\mathrm{MOS_{OV}} = \left(1 - \frac{\mathrm{MOS}}{5}\right) \times 100\% \tag{19}$$

The time complexity of an algorithm is a figure of merit that measures the variation in the runtime of an algorithm with the size of the input data. In the proposed algorithm, the runtime mainly depends on three parameters (i) the down-sampling factor, (ii) α_{opt}, and (iii) β_{opt}. The values of α_{opt} and β_{opt} entirely depend on the correlation that is present among the MECG leads, and therefore, it is diffi-

Table 4
MOS errors of various features and over MECG.

Features	MOS (%) error		Features	MOS (%) error	
	MOS_{Fe}	MOS_{OV}		MOS_{Fe}	MOS_{OV}
QRS-amplitude	3.33	6.33	P-wave amplitude	11.67	
QRS-shape	3.33		P-wave polarity	3.33	6.33
QRS-duration	3.33		P-wave duration	11.33	
T-wave amplitude	6.67		ST-elevation	3.33	
T-wave polarity	3.33		PR-interval	3.33	
T-wave duration	3.33		QT-interval	3.33	

cult to quantify the time complexity of this proposed algorithm. However, the mean time-complexity of the proposed algorithm calculated using all 549 MECG signals of PTBDB with different sizes of patient-information data is shown in Fig. 8. From this figure, it can be seen that the time-complexity of the *QSMECGcomp* algorithm (i) varies approximately linearly with the length of the MECG signals, (ii) though minor, increases with the size of the patient-information data, and (iii) the reconstruction time of the MECG data is significantly lower than its compression. In this research, the algorithm is implemented on a software platform and therefore, the power-requirement is not considered in this paper. The algorithm is developed on MATLAB R2018a platform with a computer running Windows 10 operating system, 16 GB RAM and Intel Xeon CPU E3–1271 v3 3.60 GHz. The computational and space complexities of the proposed algorithm are summarized in Table 5.

Note that although the time complexities of both DCT and inverse-DCT are O(*rc* log *rc)*, following the asymptotic nature of the Big-O notation, the term O(*rc* log *rc)* is considered only once. Similarly, both the terms O(*rc)* and O(*λc)* appear twice but are considered once in the expression of space complexity. The total time complexity can thus be expressed as:

$$Totaltimecomplexity = O\left(rclogrc + \lambda c^2 + \lambda c^3 + rc\right) \tag{20}$$

As the term *rc* log *rc* dominates *rc* and λc^3 dominates λc^2, the equation simplifies to:

$$Totaltimecomplexity\,(simplified) = O\left(rclogrc + \lambda c^3\right) \tag{21}$$

It is also to note that the equations of time (Eqs. (20) and (21)), and space complexities are linear. Fig. 9 shows the plot of time (Eq. (20)) and space complexities as a function of the number of rows *r* and DCT truncation factor α setting $c = 8$.

The performance of a biosignal-steganography algorithm can be quantified using a technique called bit-error-rate [24], which calculates the percent of erroneous, modified or lost bits in the patient's confidential information data upon reconstruction. Bit-error-rate is expressed as

$$R_{BE} = \frac{b_{err}}{b_{total}}\,(\%) \tag{22}$$

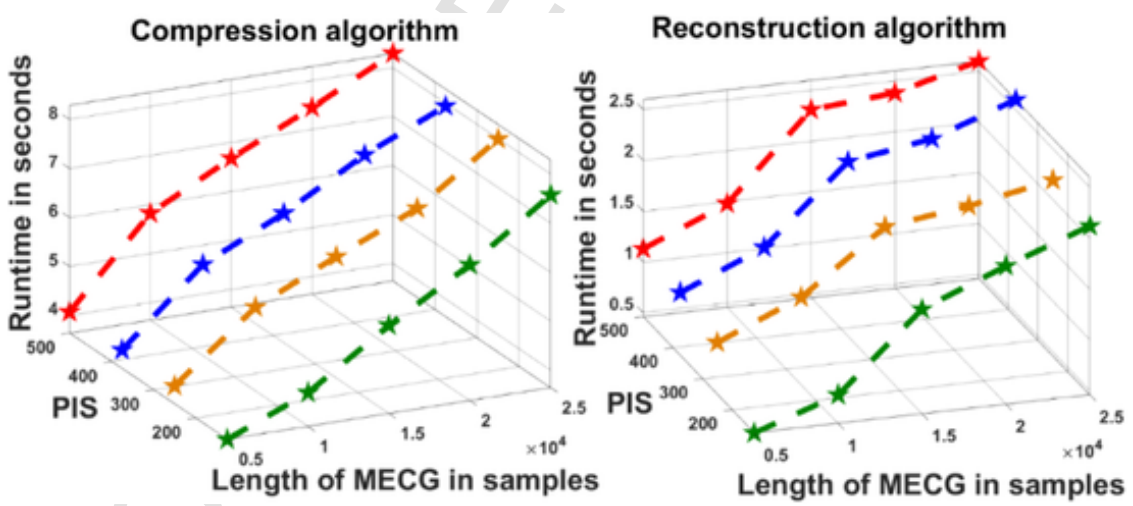

Fig. 8. (Left) Time-complexity of the proposed *QSMECGcomp* algorithm, (Right) Time-complexity of the reconstruction algorithm. PIS→ patient-information data size.

Table 5
Calculation of computational and space complexities.

Computational complexity calculation			Space complexity calculation		
r is the number of rows and *c* is the number of columns of the *MECG* matrix, and λ is α % of *r*. The value of β_{opt}, i.e., the number of columns, c, vary from 1 to 8.					
Step	Operation	Time complexity	Variable	Size	Memory
DCT	$MDCT_{r\times 8} \leftarrow DCT2(MECG_{r\times 8})$	O(*rc* log *rc)*	Input ECG	*rc*	O(*rc)*
SVD on λ × *c* matrix	$U_{\lambda\times\lambda}\,S_{\lambda\times c}\,V^T_{c\times c} \leftarrow SVD\,(Temp_{\lambda\times c})$	$O(\lambda c^2)$	DCT result	*rc*	O(*rc)*
Reconstruction loop (1 to c)	β_{opt} SVD truncations	$O(\lambda\beta_{opt}c^2) = O(\lambda c^3)$	DCT result	λ*c*	O(λ*c)*
Inverse DCT	$\overline{MECG_{r\times 8}} \leftarrow iDCT2\,(Z)$	O(*rc* log *rc)*	SVD outputs	*U, S, V*	$O(\lambda c + c^2)$
PRD and WEDD computation	Vector operations	O(*rc)*	Reconstruction	λ*c*	O(λ*c)*
Total $O(rc \log rc + \lambda c^2 + \lambda c^3 + rc)$			Total $O(\lambda c + rc + c^2)$		

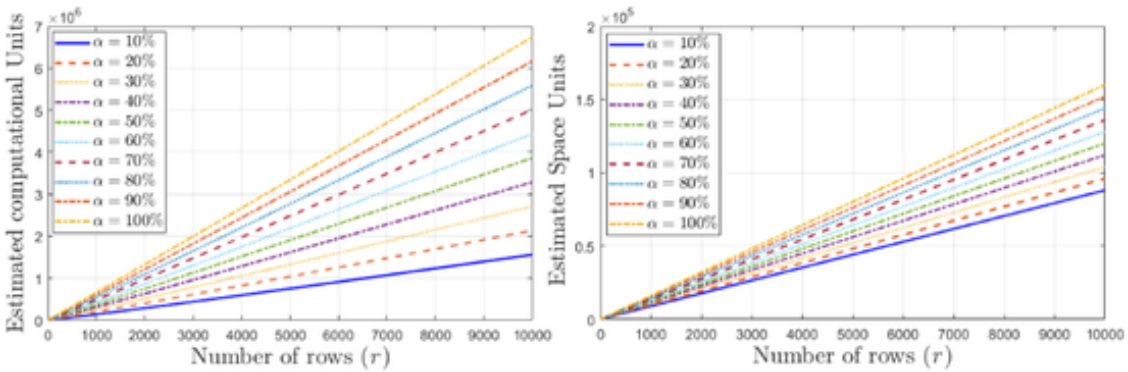

Fig. 9. Plot of time (Eq. (20)) (left) and space (right) complexities as a function of the number of rows r and DCT truncation factor α (%) setting $c = 8$.

where b_{err} is the total number of erroneous bits found upon reconstruction, and b_{total} is the total number of bits in the original data. In this research, patient's personal data is compressed and reconstructed along with the $U_{\alpha_{opt}\times\beta_{opt}}$ matrix coefficients using a lossless ASCII character encoding-based technique (please see Fig. 4A–C). Therefore, R_{BE} is always zero in this research. Also, the MECG reconstruction error does not depend on the steganographic data.

6. Analysis of security

The proposed *QSMECGcomp* algorithm generates four files, ASCIIdiff.dat, CECG.dat, Vcoeff.dat and SecKey.dat., at four different stages of the algorithm. In the first-difference of the $\widetilde{U}$ matrix coefficients if any data value is found to be greater than 255, it is replaced with 255, and the corresponding data-value and its index are stored in a file named 'ASCIIdiff.dat'. The file CECG.dat contains the compressed MECG signal, the quantized right singular matrix ($V^T_{8\times\beta_{opt}}$) coefficients are stored in the file Vcoeff.dat, and the file SecKey.dat contains the security keys. Fig. 10 shows an exemplary content of these files.

Security analysis of *Vcoeff.dat*: Deletion of any part of the data from this file prevents the reconstruction algorithm from executing. To faithfully reconstruct the $V^T_{8\times\beta_{opt}}$ matrix, the algorithm requires the exact data size in the *Vcoeff.dat* file as well as the maximum and minimum values of the $V^T_{8\times\beta_{opt}}$ matrix coefficients. Moreover, if an intruder modifies the file, the reconstructed signal will no longer resemble a valid ECG. To simulate this, the characters 'Fum' (as shown in Fig. 10) are altered to 'ABC', and the maximum value of the $V^T_{8\times\beta_{opt}}$ matrix coefficients (i.e., 0.987) is replaced with an arbitrary value of 0.123. Fig. 11A illustrates the impact of these changes on the output signal. Visual inspection alone indicates that the file has been tampered with.

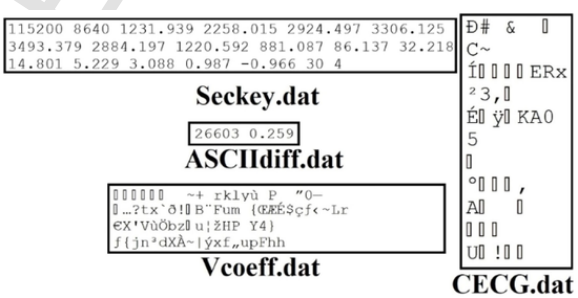

Fig. 10. Exemplary content of *ASCIIdiff.dat, CECG.dat, Vcoeff.dat, and* Sec*Key.dat* files.

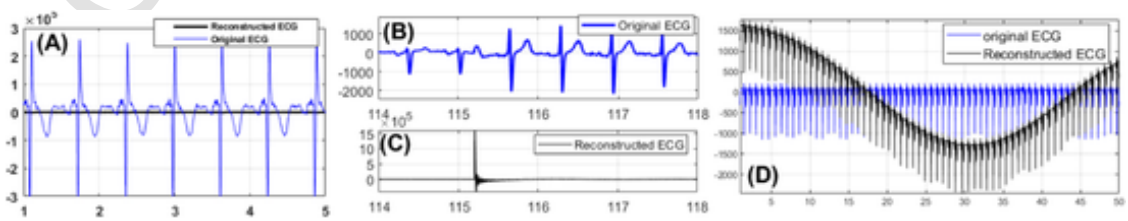

Fig. 11. (A) Impact of tampering in the *Vcoeff.dat* file. (B, C) Impact of tampering in the *ASCIIdiff.dat* file, and (D) Impact of tampering in the *CECG.dat* file.

Security analysis of *ASCIIdiff.dat*: The effect of deletion or tempering with the content of this file has a significant impact on reconstruction quality. To simulate this, the numbers 26603 and 0.259 (as shown in Fig. 10) are replaced with arbitrary values, 158 and 0.503, Fig. 11B and 11C illustrate the impact of these changes on the output signal. Visual inspection alone confirms that the file has been tampered with.

Security analysis of *CECG.dat*: Deletion of any part of the data in this file prevents the reconstruction algorithm from executing. However, any attempt to tamper with the data can be easily detected from the reconstructed signal. To simulate this, a few randomly chosen characters from the *CECG.dat* file (as shown in Fig. 10) are replaced with other characters. Fig. 11D illustrates the impact of these changes on the output signal, showing significant distortion and baseline modulation. Since baseline wander noise has already been removed from the original MECG signal during preprocessing, its presence in the output clearly indicates an attempt of data tampering.

Security analysis of Sec*Key.dat*: Seven entities have been selected in this research to serve as components of the security key: (1) the down-sampling factor *D*, (2) *r* (3) $ANF_{1\times 8}$ (4) α_{opt}, (5) the number of rows *n* in the *PCI* matrix, (6) maximum and minimum values of the $V^T_{8\times\beta_{opt}}$ matrix coefficients, and (7) β_{opt} singular values. Among these, (i) deletion of any of the entity or (ii) tempering with the values of *r*, α_{opt}, *n*, prevents the reconstruction algorithm from executing. The adverse effect of tempering with the maximum and minimum values of the $V^T_{8\times\beta_{opt}}$ matrix coefficients is already shown in Fig. 11A. However, a tempering the values of *D*, $ANF_{1\times 8}$ and β_{opt} might alter the morphology of the ECG signal. For example, (i) if the down-sampling factor *D* is modified, the resulting ECG signal may exhibit an abnormally high or low heart rate, and (ii) if the $ANF_{1\times 8}$ or singular values are changed, the amplitude of the ECG signal may change, potentially leading to an incorrect diagnosis.

We have also evaluated the security of the proposed steganographed MECG compression scheme using both entropy and Regular-Singular steganalysis in the transform domain. Regular-Singular steganalysis is a statistical method that detects hidden information by analyzing changes in smoothness patterns of regular and singular groups in the transform domain. The entropy of the $U_{\alpha_{opt}\times\beta_{opt}}$ matrix coefficients (i.e., before steganography) has been 4.2684 bits, while the entropy of the as $\widetilde{U}$ matrix coefficients (i.e., after steganography with PI = 500 bytes) has been 4.3908 bits, indicating only a minor increase in randomness. Regular-Singular analysis shows that the original coefficients produced 12,370 regular and 1926 singular groups, whereas the steganographed coefficients yielded 12,555 regular and 2005 singular groups. The marginal differences ($\Delta R = 185$, $\Delta S = 79$), corresponding to relative changes of 1.5% and 4.1%, respectively, indicate that the embedding process has not significantly altered the smoothness patterns in the transform domain. Moreover, the histogram plots, in Fig. 12, of the $U_{\alpha_{opt}\times\beta_{opt}}$ matrix coefficients before and after steganography further confirm that the coefficient distributions remain nearly unchanged. Therefore, the entropy, Regular-Singular analysis, and histogram results demonstrate that the proposed method preserves the statistical properties of the coefficients and remains highly undetectable to potential intruders.

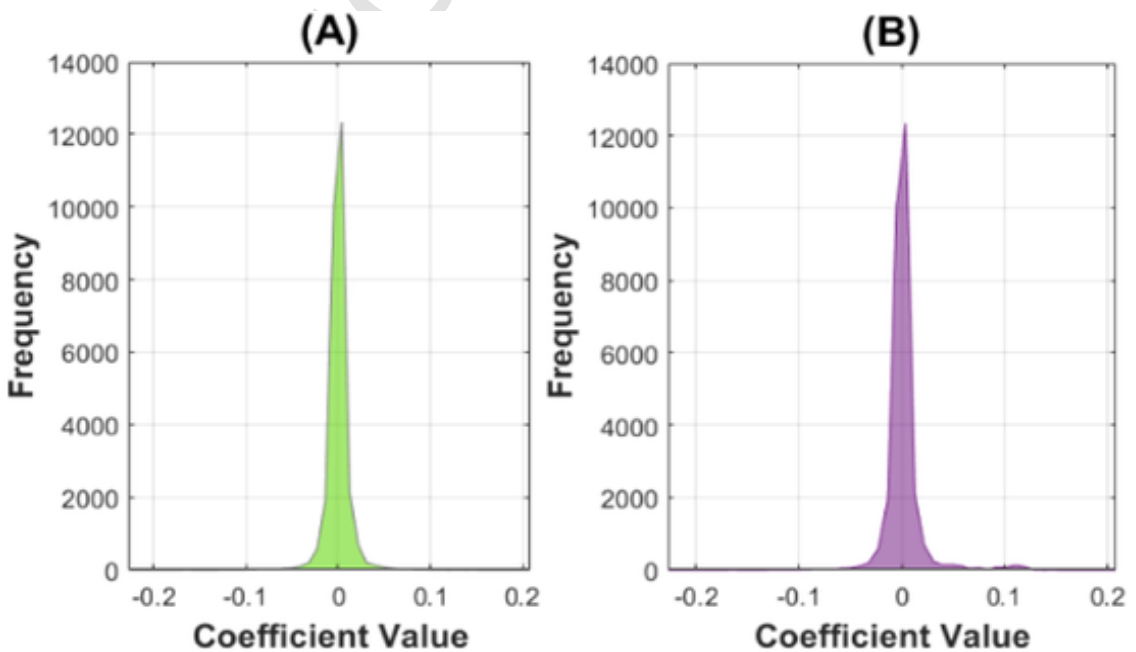

Fig. 12. Histogram plots of the $U_{\alpha_{opt}\times\beta_{opt}}$ matrix coefficients before (A) and after (B) steganography. The distributions remain nearly identical.

Section 3.5 has demonstrated that the probability of successfully guessing the security key values is extremely low. However, an event of data breach or tampering could lead to an incorrect diagnosis. Strategies to prevent data breaches, contain the impact through sandboxing, and encrypt the security keys themselves will be explored in our future research.

7. Performance comparison

In this Section, first, the performance of the proposed *QSMECGcomp* algorithm is compared to that of another similar type of algorithm [16] available in the literature to date, where a quality guaranteed steganographed MECG compression algorithm is proposed. Then, the proposed algorithm is (i) revamped and reconfigured excluding the steganography operation, and (ii) its performance is reevaluated on the MECG signals so as to compare its performance with that of other MECG compression algorithms only available in the literature. We shall call this reconfigured algorithm as '*MECGComp*'. The values of the performance evaluation metrics of other algorithms are taken from the respective literature.

It has been found in the literature that a few other metrics such as percent root mean square difference (PRD), normalized PRD (PRDN), and quality score (QS) [32] along with WEDD have also been used to quantify the reconstruction performance of the MECG signals. As per the globally considered standard [33], the quality of the reconstructed ECG/MECG signal is considered to be 'very good' if the PRD values lies within the range 0 to 2%, 'good' if it lies within the range 2% to 9%, 'not good' if it lies within the range 9% to 19%, and 'bad' if it is found to be $>19\%$.

The algorithm [16] achieves a maximum compression ratio of 63.7 for a group of 16 MECG signals (which are labelled as dysrhythmia) taken from PTBDB with an average PRD value of 9.3%. The modifications which have been done so as to compare the performance of the proposed *QSMECGcomp* algorithm with that of [16] are (i) MECG reconstruction performance is quantified using PRD instead of WEDD, and (ii) the optimum values of α_{opt} and β_{opt} are calculated in such a way that the average PRD value of all the ECG leads would not exceed Th_{UD} upon reconstruction. The performance of the proposed *QSMECGcomp* algorithm is compared to [16] in Table 6.

It is interesting to note that, it has been tried in [16] to limit the average PRD value to 5% upon reconstruction. However, for the dysrhythmia group the average PRD value of [16] reaches 9.3% upon reconstruction, which is not only 4.3% more than that of the threshold, but also as per the gold-standard PRD criteria the reconstructed MECG signals fall under the category 'not good'. When comparing our proposed algorithm to [16], we set the values of Th_{UD} to 9.3% and 5.59% to closely-match the level of the MECG reconstruction error with that of [16] and then comparing the corresponding values of the CR. It can be seen in Table 6 that, for the dysrhythmia group of MECG signals the CR of the proposed algorithm is about ~2.52 times better than that of [16]. In [16], the authors have also claimed that the CR values are reported including the steganographic information, but the size of the patient-information data is not mentioned. The runtime of the algorithm [16] is calculated using a CPU which is much faster than that of the one used in this research. Nevertheless, the proposed algorithm is about ~21.59 times faster than that of [16].

Now, the performance of the proposed *MECGComp* algorithm is compared to other MECG compression algorithms in Table 7. Compared to single-lead ECG, relatively few multi-lead ECG (MECG) compression algorithms have been proposed in the literature to date. Among these, most are based on the compressive sensing framework. ECG and MECG signals are sparse in nature. CS leverages this sparsity to reconstruct signals using even fewer samples than that of Nyquist sampling would require. CS-based techniques are popular for MECG compression because they exploit both intra-lead and inter-lead sparsity, enabling efficient sensing and transmission. These characteristics make CS particularly well-suited for wearable and remote monitoring applications. However, as reported in the literature, the compression ratios achieved by CS-based frameworks are generally lower than those of WT, SVD, and DCT-based methods. Table 7 compares the performance of twelve algorithms, six of which are CS-based. Among these six, four algorithms [8–10,12] achieve a CR of less than 15. Algorithm [11] performs moderately better, and algorithm [16] offers an exceptionally high compression ratio of 58.51 compared to the other five CS-based approaches. Moreover, except [11,8], the remaining four CS-based methods demonstrate low MECG reconstruction errors. The operation of the algorithms proposed in [18,20,14,15,17] is similar to that of the proposed algorithm, where the ECG signal is first decomposed into low-rank components, which are then further compressed using various techniques such as Huffman coding [18,20,15] and delta encoding [17]. The number of prediction-based algorithms proposed in the ECG compression literature is very limited, and algorithm [21] is one such example. The working principle of prediction-based algorithms differs significantly from that of CS and decomposition-based approaches.

The performance of the proposed *MECGcomp* algorithm is evaluated on all the 549 MECG signals of PTBDB totaling a duration of 16.03 h and the average values of the performance-evaluation metrics are reported in Table 7. Performance-evaluation metrics of all

Table 6
Performance comparison between *QSMECGcomp* and [16].

Data and database	Algorithm	Patient information	Th_{UD} in PRD (%)	ǂMean PRD (%)	Mean CR	Mean QS	Time-complexity
16 MECG data files of dysrhythmia group, PTBDB	[16]	Not mentioned	5.00	9.30	63.7	6.85	12.74μs/sample (Intel Core i5 CPU, 3.19 GHz; (↑) MATLAB)
546 MECG data files, PTBDB	[16]	Not mentioned	5.00	5.59	55.40	9.84	
16 MECG data files of dysrhythmia group, PTBDB	Proposed	500bytes	9.30	**8.18**	**160.82**	**19.66**	**0.59**μs/sample (CPU E3–1271 v3, 3.60 GHz)
546 MECG data files, PTBDB	Proposed	500bytes	5.59	**5.30**	**98.84**	**18.65**	

ǂ PRD is calculated upon MECG reconstruction. ↑ superior CPU.

Table 7
Performance comparison between *MECGcomp* and other MECG compression algorithms.

Algorithm	Th_{UD} in PRD (%)	PRD (%)	WEDD (%)	CR	QS	CPU specification	Time-complexity
CS-based algorithms							
CS [9]	NC	5.13	NC	8.00	1.56	Intel Core i7, 3.40 GHz. (↑)	4.14 s for 224 samples
CS [8]	NC	9.14	NC	8.00	0.88	Intel Core i7, 3.40 GHz. (↑)	Compression→422 s for 28,992 × 12 samples (28.992 s of MECG)
CS [10]	NC	~6	NC	10.00	1.67	Intel Core2Duo, 2.53 GHz, P8700. (↓)	Compression→0.061 s for 500 samples
CS [12]	NC	5.29	2.35	13.91	3.39	Intel Core i5, 3.20 GHz. (↑)	Compression→0.53 s, reconstruction→2.41 s for 300 × 8 samples
CS [11]	NC	13.60	10.71	27.31	2.01	3.1 GHz CPU (↓)	Compression→12.781 s for 512 × 8 samples
CS [13]	NC	6.60	6.07	58.51	8.87	Intel Core i5, 3.20 GHz. (↑)	Compression→0.16 s, reconstruction→6.48 s for 3000 × 8 samples
Decomposition/transformation-based algorithms							
PCA [18]	NC	2.09	7.23	5.98	3.46	NM	NM
SVD [20]	NC	6.67	2.67	22.10	3.31	Intel Core i5, 3.20 GHz. (↑)	Compression→1.08 s for 4096 × 8 samples
Tensor [14]	NC	8.35	NC	43.05	5.94	Intel Core i5, 1.8 GHz. (↑)	Compression→0.24 s
Tensor [15]	NC	2.71	**2.01**	45.00	16.61	Intel Core i5, 3.20 GHz. (↑)	NM
Fourier [17]	3.00	3.88	NC	48.21	12.43	Intel Core i5, 3.19 GHz. (↑)	NM
Prediction-based algorithm							
Prediction [21]	NC	NM	NC	4.073	–	Hardware	NM
Proposed	4.00	**3.85**	2.30	**71.87**	**18.67**	Intel E3–1271 v3, 3.60 GHz	Compression→26.79 s, reconstruction→12.5 s for 120,012 × 8 samples
	5.50	**5.23**	**3.12**	**100.45**	**19.21**		
	9.00	**8.29**	**4.86**	**160.35**	**19.34**		

↑ superior CPU, ↓ inferior CPU, NM= not mentioned, NC = not calculated.

the algorithms (except [18]), which are mentioned in Table 7 are evaluated on the MECG signals taken from PTBDB. In [18], the performance is evaluated on CSE multi-lead ECG database. The CSE database is not available publicly, and hence, the performance of the proposed *MECGcomp* algorithm is not evaluated on this database. The adaptive linear prediction-based MECG signal compression algorithm proposed in [21] has been implemented on hardware platform and the time-complexity is not mentioned. Therefore, it is not possible to compare the runtime of the proposed algorithm with that of [21]. As the average PRD value of the reconstructed MECG signals is not mentioned in [21], it is also not possible to compare the reconstruction quality of the proposed algorithm with that of [21]. However, in terms of CR, our proposed *MECGcomp* algorithm ace [21].

In [8], the CR and PRD values are evaluated on MECG signals totaling a duration of 290 s (~4.83 min) only. The algorithm [8] achieves an average CR of 8 with an average PRD value of 9.14%. For around a similar value of PRD (even less) of 8.29% (Th_{UD} = 9%), our proposed *MECGcomp* algorithm offers an average CR value of 160.35, which is around ~20.04 times better than that of [8]. Even though the algorithm [8] is implemented, and the runtime is calculated using a CPU which is superior to that of ours, the proposed *MECGcomp* algorithm can process the same number of MECG samples much faster compared to that of the one in [8].

The algorithm proposed in [10] offers an average CR of 10 against an average PRD value of ~6%. For around the similar PRD value (even less) of 5.23%, our proposed *MECGcomp* algorithm offers a compression ratio of 100.45, which is about ~10.05 times better than that of the one in [10]. The algorithm [10] is implemented, and the runtime is calculated using a CPU which is weaker than that of the one which is used in our research. Therefore, a direct comparison of the runtimes with [10] would not be an apt.

The average value of PRD reported in [12] (5.29%) and the average PRD value obtained using *MECGcomp* (PRD = 5.23% for Th_{UD} = 5.5%) are very close. However, for such similar values of PRD our proposed *MECGcomp* algorithm offers a CR which is about ~7.22 times better than that of the one in [12]. The algorithm [12] achieves an average value of WEDD of 2.35% which is 0.77% better than that of our proposed algorithm. To compress and reconstruct 300 × 8 MECG samples the algorithm [12] takes 0.53 s and 2.41 s, respectively. Whereas our proposed *MECGcomp* algorithm takes 0.19 s and 0.01 s, respectively, to compress and reconstruct the same number of MECG samples.

The tensor decomposition-based MECG compression algorithm proposed in [14] achieves an average CR of about 43.05 ± 2.01 against an average value of PRD of 8.35% ± 2.28%. For around a similar value of PRD of 8.29% (Th_{UD} = 9%), our proposed *MECGcomp* algorithm offers an average CR of 160.35, which is about ~3.72 times better than that of the one in [14]. The average runtime of the algorithm [14] is mentioned to be 0.24 s, but the data size is not mentioned. Instead of processing the total length of the MECG signals at once, the algorithm [14] breaks down the input MECG signal into chunks and processes one chuck at a time.

The adaptive Fourier decomposition-based MECG compression algorithm proposed in [17] achieves and average CR of about 48.21. It has been tried in [17] to keep the PRD value below 3% upon reconstruction. However, the average value of PRD in [17] reached 3.88% upon reconstruction, which is not an apt example of a good quality control. For such a similar average value of PRD of 3.85% (Th_{UD} = 4%) our proposed *MECGcomp* algorithm offers an average CR of 71.87. Runtime of the algorithm [17] is not mentioned.

Out of these 12 MECG compression algorithms which are compared in Table 7 (i) one of the algorithms [21] is implemented on hardware platform, (ii) the CPU specification on which one of the algorithms [18] is implemented is not mentioned, (iii) 8 of the algo-

rithms are implemented on CPUs which are mightier than that of the one used in implementing the proposed algorithm, and (iv) 2 of the algorithms [10,11] are implemented on CPUs which are weaker than that of the one used in implementing the proposed algorithm. The QS of our proposed algorithm is better than all other algorithms compared in Table 7.

As described in Section 5, (i) R_{BE} of the proposed *QSMECGcomp* algorithm is zero, and also (ii) the error in the reconstructed MECG signals is introduced mostly due to the DCT, SVD and up/down-sampling operations and not for the steganography operation (please see Table 3). This can also be noted from Table 3, that the value of the CR changes with the size of the patient-information data but the values of ME_P and ME_R remain constant for a particular database. Therefore, it can be said that the contribution of the steganography operation to PRD or WEDD is zero. Steganographic performance of the proposed *QSMECGcomp* algorithm is compared with a few other algorithms in Table 8.

From Table 8, it can be seen that the algorithms [23–25,35], which are developed solely for the purpose of ECG/MECG steganography introduce, though trivial, error in the reconstructed signals. However, the MECG reconstruction error because of the steganography operation in our proposed *QSMECGcomp* algorithm is zero.

8. Discussion

Percent root mean square difference (PRD), as expressed in Eq. (23), is a measure of distortion between the original and reconstructed ECG signals in time-domain. In calculating PRD, the amplitude of every reconstructed ECG-sample is compared to its original counterpart. On the other hand, WEDD is a measure of distortion between the original and reconstructed ECG signals in frequency-domain. In the calculation of WEDD, both the original and reconstructed ECG signals are decomposed into multiple approximation and detail frequency bands using wavelet transform, and the distortion is then measured, like PRD, between the corresponding paired frequency bands. Both amplitude and frequency components are integral to an ECG signal, and an ideal algorithm should preserve both. In the domain of ECG signal processing, in addition to PRD and WEDD, several other quality estimation metrics are commonly used such as mean squared error (MSE), root mean square error (RMSE), mean absolute error (MAE), and signal-to-noise ratio (SNR). However, unlike PRD and WEDD, the interpretation of these metrics for ECG signals has not yet been standardized. In developing the *QSMECGcomp* algorithm, WEDD has been chosen as the primary measure of quality in this research. However, (i) PRD can also be used interchangeably, and (ii) both WEDD and PRD may be used together for a more comprehensive assessment. Fig. 13A and 13B exemplify the notion. For this reconstructed ECG signal MSE, RMSE, MAE and SNR are calculated along with WEDD and PRD.

$$\mathrm{PRD}\,(\%) = \sqrt{\frac{\sum_{i=1}^{n}\left(x_i - \hat{x}_i\right)^2}{x_i^2}} \times 100 \tag{23}$$

Table 8
Comparison of steganographic performance.

Algorithm	R_{BE} (%)	PRD (%) due to steganography
LSTM [23]	0	0.005 - 0.035
Golay Code [24]	0	0.006 - 0.009
Deep learning [35]	0	0 - 0.89
Walsh–Hadamard [25]	0	0.487 – 0.524
Proposed	0	**0**

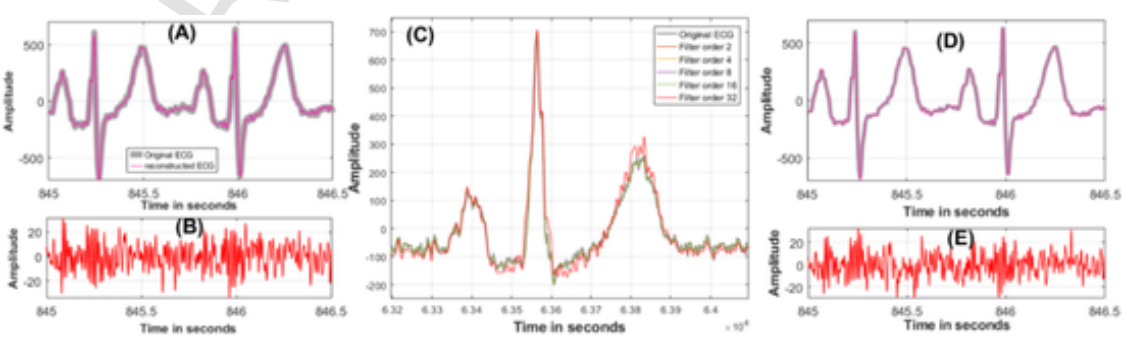

Fig. 13. (A) Original (preprocessed using a 4th order Butterworth filter) and reconstructed ECG signals of Lead V6, File# s0216, PTB-DB, (B) error between the original and reconstructed ECG signals. PRD = 4.65%, WEDD = 2.53%, MSE = 107.50, RMSE = 10.37, MAE = 8.15, and SNR = 26.66 dB. (C) Effect of increasing the order of the filter. (D) Original (preprocessed using a 2nd order Butterworth filter) and reconstructed ECG signals of Lead V6, File# s0216, PTB-DB, (C) error between the original and reconstructed ECG signals shown in (E). PRD = 4.649%, WEDD = 2.53%, MSE = 107.37, RMSE = 10.3607, MAE = 8.15, and SNR = 26.65 dB.

$$\mathrm{MSE} = \frac{1}{n}\sum_{i=1}^{n}\left(x_i - \hat{x}_i\right)^2 \tag{24}$$

$$\mathrm{RMSE} = \sqrt{\mathrm{MSE}} \tag{25}$$

$$\mathrm{MAE} = \frac{1}{n}\sum_{i=1}^{n}\left|x_i - \hat{x}_i\right| \tag{26}$$

$$\mathrm{SNR\,(dB)} = 10\log_{10}\left(\frac{\sum_{i=1}^{n} x_i^2}{\sum_{i=1}^{n}\left(x_i - \hat{x}_i\right)^2}\right) \tag{27}$$

where x_i is an original ECG sample, $\hat{x}_i$ is the corresponding reconstructed sample, and n is the total number of samples in the signal. It has also been shown in [38], that SNR can be calculated from the PRD value as follows.

$$\mathrm{SNR\,(dB)} = -20\log_{10}(0.01 \times \mathrm{PRD}) \tag{28}$$

The performance of the proposed method is compared with twelve other algorithms, as presented in Table 7. Among these, (i) only two algorithms, those proposed in [12,13], report SNR values alongside PRD; (ii) six algorithms report WEDD in addition to PRD; and (iii) four algorithms report only PRD. In [12,13], the average SNRs reported for the PTB-DB are 23.99 dB and 23.67 dB, respectively. In the present study, the average SNR is found to be 28.32 ± 0.05 dB and 21.63 ± 0.06 dB for Th_{UD} PRD values of 4.00% and 9.00%, respectively.

Removing high and low-frequency noise from ECG signals during the preprocessing stage is a prerequisite—not only for compression algorithms but also for algorithms that detect cardiac abnormalities from ECG signals [15,18,20,14]. In [15,18,20], wavelet-based filtering techniques have been used, while [14] employs a Savitzky-Golay filter. Increasing the filter order helps suppress noise components; however, higher-order filters may also distort the morphology of the signal, as demonstrated in Fig. 13C. From this figure, it can be observed that increasing the filter order up to 16 effectively suppresses the high-frequency noise. However, beyond this point, the ECG signal begins to lose its clinical morphology. Choosing the appropriate order of the filter is critical and depends on the length of the input signal. If the signal is too short, a high-order filter may distort it; conversely, if the signal is long, a low-order filter may be ineffective in removing noise. A practical guideline commonly followed in digital signal processing suggests that the signal length should be at least an order of magnitude greater than the order of the filter to ensure stable and accurate filtering, particularly for IIR filters. As shown in Table 2, the ECG signals used in this study are significantly longer. Therefore, the use of a 4th-order bidirectional Butterworth filter does not distort the clinical morphology in this research. Moreover, the use of a 4th-order Butterworth filter for ECG noise removal has also been reported in [39]. In Fig. 13A, and ECG signal is compressed and reconstructed using after 4th order Butterworth filter. The same signal is now processed using a 2nd order Butterworth filter, and the result is shown in Fig. 13D and 13E. It can be seen that the difference in the performance metrics is trivial.

Discrete cosine transform (DCT), singular value decomposition (SVD), down sampling, quantization, and ASCII character encoding are the main building blocks of the proposed algorithm. Except the ASCII character encoding technique, which is a lossless one, rest of the techniques are lossy in nature. It is seen in our research that most of the signal reconstruction error is introduced due to the DCT and SVD operations. Fig. 14A–14D shows the reconstruction error that is introduced to the signal due to the down sampling operation. The ECG data is taken from PTB-DB (sampling rate 1 kHz) and down-sampled by a factor of 4. Then the signal is restored back

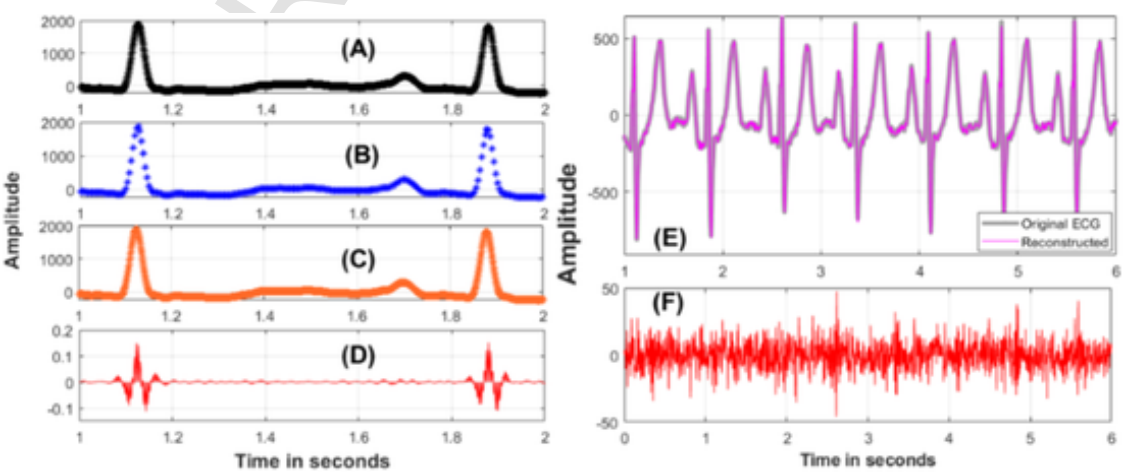

Fig. 14. (A) original ECG signal; File# s0216, PTB-DB, (B) down-sampled signal by a factor of 4, (C) up-sampled signal, (D) amplitude difference between the signals shown in (A) and (C). PRD = 0.0049%, WEDD = 0.0025%, (E) original and reconstructed signals on top of each other, (F) reconstruction error due to down-sampling (factor = 4), DCT (α_{opt} = 50% coefficients) and SVD (β_{opt} = 5) operations only. The corresponding PRD = 4.53%, and WEDD = 2.58%.

to its original sampling rate. It can be seen from the figure that the scale of the amplitude of the error signal (Fig. 13D) is of the order of $\sim 10^{-4}$ of the original one. Moreover, the PRD and WEDD values that are obtained due to the down-sampling operation, are 0.0049% and 0.0025%, respectively-which are very small.

Now the reconstruction error that is introduced due to down-sampling (factor = 4), DCT (α_{opt} = 50% coefficients), SVD (β_{opt} = 5) operations are shown in Fig. 14E and 14F. It can be seen that the values of predicted PRD and WEDD are 4.53% and 2.58% respectively. Moreover, the actual values of PRD and WEDD upon reconstruction are found to be 4.532%, and 2.58006%, respectively. Therefore, the reconstruction error due to the quantization operation increases the PRD value by an amount ~0.002%, which is ~93.98 dB. The PRD and WEDD values are obtained for a user-defined WEDD value of the error-threshold (Th_{UD}) of 6.914%, and it could further be reduced by setting Th_{UD} to a lower value of WEDD.

The Discrete Cosine Transform (DCT) has been used in this research due to its excellent energy compaction property - that is, the total energy of the MECG matrix is concentrated into a smaller number of DCT coefficients, as illustrated in Fig. 2. Other transforms known for effective energy compaction, such as the wavelet transform, Karhunen–Loève transform, and principal component analysis, can also be considered. These alternatives will be explored in future research.

Although several lossless compression techniques such as Huffman coding and Run-Length Encoding (RLE) are available, this research employs an ASCII character encoding-based lossless compression method. The primary motivation behind this choice is its superior compression performance. Huffman coding typically offers a compression ratio of approximately 3, while Run-Length Encoding achieves around 5; both under conditions of highly repetitive data. ECG signals are quasi-repetitive in nature, but in this study ASCII encoding is applied to the truncated-SVD data of DCT coefficients combined with patient confidential information, which is significantly less repetitive than the MECG itself. Moreover, the ASCII encoding technique achieves a compression ratio of approximately 10. Future work will explore whether applying Huffman or Run-Length Encoding on top of the ASCII-compressed data can further reduce the overall data size.

As described in Section 3.2, the process begins by selecting only 10% of the total DCT coefficients. The number of DCT coefficients is increased by 10% in each iteration, and in each iteration, the number of singular values varies from 1 to 8. For example, suppose an MECG signal requires at least 18% of the DCT coefficients to achieve a WEDD or PRD below the threshold Th_{UD} upon reconstruction. In this case, since the increment is 10%, convergence will occur in the 2nd iteration, i.e., at 20% of the DCT coefficients. Increasing the DCT increment factor (e.g., from 10% to 25%) results in faster convergence but a lower compression ratio. Conversely, decreasing the increment factor (e.g., from 10% to 1%) leads to longer convergence time but with precise control over the reconstruction error. Fig. 15 illustrates this process, showing the variation of WEDD and PRD across iterations as a function of the percentage of DCT coefficients and the number of singular values for ECG File #s0274 from the PTB-DB. Since the number of singular values starts from 1 in each iteration, both PRD and WEDD begin at higher values and decrease gradually. Fig. 15A shows that decreasing the DCT-coefficients incremental-factor will provide precise control over the reconstruction error at the cost of increased convergence time, while increasing the incremental-factor leads to faster convergence (Fig. 15C) but results in a lower compression ratio. Therefore, the DCT-coefficients incremental factor is set to 10% in this research work.

9. Conclusion

The proposed research addresses quality-guaranteed compression of MECG signals combined with steganography. The proposed algorithm introduces two main improvements: (i) significantly higher compression performance compared to existing methods, and (ii) robust, reliable, lossless, and highly secure steganography. Filtering and arranging the eight ECG leads properly while forming the $MECG_{r \times 8}$ matrix increases intra- and inter-lead correlation, improving compression. Experimental results show that if the lead order is not maintained, both the compression ratio drops and the reconstruction error rises. For instance, compressing File#s0001 of PTBDB with 500 bytes of patient information while maintaining the ECG lead order (V1-V6, I, II) using *QSMECGcomp* yields a compression ratio of 134.28 and a WEDD of 6.85%. Randomizing the lead order gives a slightly lower ratio of 133.98 and WEDD of 6.86%.

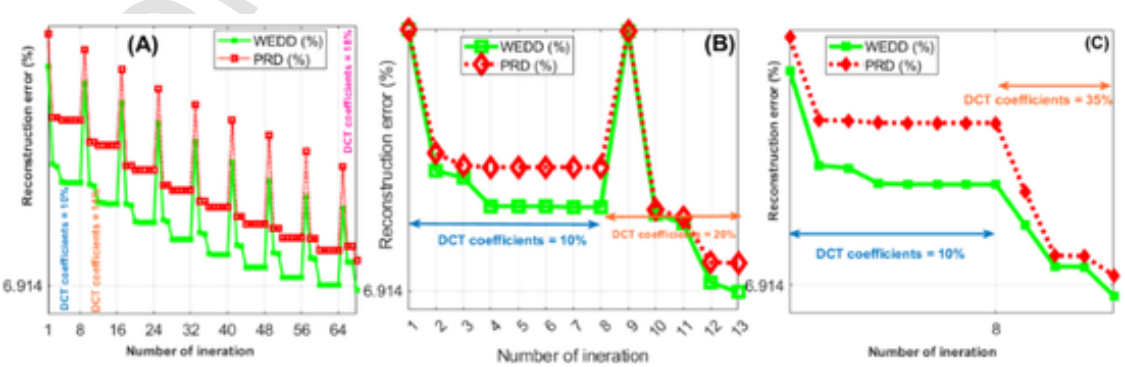

Fig. 15. Plot of reconstruction error as a function of iteration. (A) the DCT-coefficient incremental factor is 1%, compression ratio =171.69, (B) the DCT-coefficient incremental factor is 10%, compression ratio = 171.67, and (C) the DCT-coefficient incremental factor is 25%, compression ratio = 151.79.

From Fig. 4A and 4D it can be seen that the magnitudes of the $\widetilde{U}$ matrix coefficients vary smoothly compared to the coefficients of the V matrix. The probability of getting a high compression ratio using the lossless ASCII character encoding-based compression technique (LL-ACE) is higher when the sample-to-sample magnitude changes gradually. This is why the V^T matrix coefficients are not compressed using the LL-ACE technique. In this research, the V^T matrix coefficients are quantized using a uniform quantizer of 2^{16} levels. Increasing the quantization levels provides more precise control over the quality of MECG reconstruction but degrades the compression ratio. A uniform quantizer of 2^{16} levels is found to be the optimum in this study. Two metrics: percent root mean square difference (PRD) and WEDD are used to numerically assess the quality of the reconstructed MECG signals. It has been experimentally observed that, in most of the cases, the ECG lead that exhibits the maximum reconstruction error according to the WEDD criteria is often different from the one identified by the PRD criteria, and vice versa.

Ethical approval

Not required.

Declaration of competing interest

The authors declare the following financial interests/personal relationships which may be considered as potential competing interests:

Sourav Kumar Mukhopadhyay reports financial support was provided by Natural Sciences and Engineering Research Council of Canada. If there are other authors, they declare that they have no known competing financial interests or personal relationships that could have appeared to influence the work reported in this paper.

Acknowledgement

The authors would like to thank many of the graduate students of the Department of Electrical, Computer, and Biomedical Engineering, Toronto Metropolitan University, for their precious time and effort in carrying out the subjective quality estimation. We would like to thank the funding provided by the Natural Sciences and Engineering Research Council (NSERC) Discovery Grant program of Canada (Grant #140853).

Data availability

The data is available online.

References

[1] Takeshita T, Yoshida M, Takei Y, Ouchi A, Hinoki A, Uchida H, Kobayashi T. Development of wearable multi-lead ECG measurement device using cubic flocked electrode. Sci Rep 2022;12(19308):1–9. article no.
[2] Statista. [Online]. Available: https://www.grandviewresearch.com/industry-analysis/smart-clothing-market-report, Accessed: Jul. 2025.
[3] Wang LH, Zhang ZH, Tsai WP, Huang PC, Angela P. Low-power multi-lead wearable ECG system with sensor data compression. IEEE Sens J 2022;22(18):18045–55.
[4] Pal HS, Kumar A, Vishwakarma A, Singh GK. Optimized tunable-Q wavelet transform-based 2-D ECG compression technique using DCT. IEEE Trans Instrum Meas 2023;72:1–13. ASN. 4006713.
[5] Tsai TH, Tung NC, Lin DB. VLSI implementation of multi-channel ECG lossless compression system. IEEE Trans Circuits Syst II Express Briefs 2021;68(8):2962–6. iss.
[6] Tang Z, Guo Y, Zhang M. A hybrid lossless ECG compressor with morphological detection and QRS prediction. In: Proceedings of the 46th annual international conference of the IEEE engineering in medicine and biology society (EMBC); 2024. p. 1–5. 15-19 Jul.
[7] Chang Y, Sobelman GE. Lightweight lossy/lossless ECG compression for medical IoT systems. IEEE Internet Things J 2024;11(7):12450–8.
[8] Deka B, Kumar S, Datta S. Dictionary learning-based multichannel ECG reconstruction using compressive sensing. IEEE Sens J 2022;22(16):16359–69. iss.
[9] Kumar S, Deka B, Datta S. Multichannel ECG compression using block-sparsity-based joint compressive sensing. Circuits Syst Signal Process 2020;39(6):6299–315. iss.
[10] Jahanshahi JA, Danyali H, Helfroush MS. Compressive sensing based the multi-channel ECG reconstruction in wireless body sensor networks. Biomed Signal Process Control 2020;61(7):1–12. iss.
[11] Singh A, Dandapat S. Weighted mixed-norm minimization based joint compressed sensing recovery of multi-channel electrocardiogram signals. Comput Electr Eng 2016;53(5):203–18. iss.
[12] Singh A, Sharma LN, Dandapat S. Multi-channel ECG data compression using compressed sensing in eigenspace. Comput Biol Med 2016;73(6):24–37. iss.
[13] Singh A, Dandapat S. Exploiting multi-scale signal information in joint compressed sensing recovery of multi-channel ECG signals. Biomed Signal Process Control 2016;29(7):53–66. iss.
[14] Xiao L, Zhang Q, Xie K, Xiao C. Online MECG compression based on incremental tensor decomposition for wearable devices. IEEE J Biomed Health Inform 2021;25(4):1041–51.
[15] Padhy S, Dandapat S. Exploiting multi-lead electrocardiogram correlations using robust third-order tensor decomposition. Healthc Technol Lett 2015;2(5):112–7.
[16] Banerjee S, Singh GK. Quality Aware compression of multilead electrocardiogram signal using 2-mode Tucker decomposition and steganography. Biomed Signal Process Control 2021;64(2):1–12. iss.
[17] Banerjee S, Singh GK. Agent-based beat-by-beat compression of 12-lead electrocardiogram signal using adaptive fourier decomposition. Biomed Signal Process Control 2022;75(7):1–9. iss.
[18] Sharma LN, Dandapat S. Multichannel ECG data compression based on multiscale principal component analysis. IEEE Trans Inf Technol Biomed 2012;16(4):730–6.
[19] Kovac O, Kromka J, Saliga J, Juskova A. Multiwavelet-based ECG compressed sensing. Measurement 2023;220(15):1–14. iss.
[20] Padhy S, Sharma LN, Dandapat S. Multilead ECG data compression using SVD in multiresolution domain. Biomed Signal Process Control 2016;23(1):10–8. iss.

[21] Tsai TH, Tsai FL. Efficient lossless compression scheme for multi-channel ECG signal processing. Biomed Signal Process Control 2020;59(5):1–8. iss.
[22] Federal Register. [Online]. Available: https://www.federalregister.gov/documents/2022/12/02/2022-25784/confidentiality-of-substance-use-disorder-sud-patient-records, Accessed: Jul. 2025.
[23] Banerjee S, Singh GK. A robust bio-signal steganography with lost-data recovery architecture using deep learning. IEEE Trans Instrum Meas 2022;71:1–10. ANS. 4007410.
[24] Rahman MS, Khalil I, Yi X. Reversible biosignal steganography approach for authenticating biosignals using extended binary golay code. IEEE J Biomed Health Inform 2021;25(1):35–46. iss.
[25] Abuadbba A, Khalil I. Walsh-Hadamard-based 3-D steganography for protecting sensitive information in point-of-care. IEEE Trans Biomed Eng 2017;64(9):2186–95.
[26] Jero ES, Ramu P, Swaminathan R. Imperceptibility-robustness tradeoff studies for ECG steganography using Continuous ant Colony Optimization. Expert Syst Appl 2016;49(7):123–35.
[27] Jero ES, Ramu P, Ramakrishnan S. ECG steganography using curvelet transform. Biomed Signal Process Control 2015;22(8):161–9. iss.
[28] Chen ST, Guo YJ, Huang HN, Kung WM, Tseng KK, Tu SY. Hiding patients confidential data in the ECG signal via a transform-domain quantization scheme. J Med Syst 2014;38(5):1–9. iss.
[29] Ibaida A, Khalil I. Wavelet-based ECG steganography for protecting patient confidential information in point-of-care systems. IEEE Trans Biomed Eng 2013;60(12):3322–30.
[30] Cetin AE, Koymen H, Aydin MC. Multichannel ECG data compression by multirate signal processing and transform domain coding techniques. IEEE Trans Biomed Eng 1993;40(5):495–9. May.
[31] Mukhopadhyay SK, Omair Ahmad M, Swamy MNS. An ECG compression algorithm with guaranteed reconstruction quality based on optimum truncation of singular values and ASCII character encoding. Biomed Signal Process Control 2018;44(6):288–306. iss.
[32] Mukhopadhyay SK, Ahmad MO, Swamy MNS. SVD and ASCII character encoding-based compression of multiple biosignals for remote Healthcare systems. IEEE Trans Biomed Circuits Syst 2018;12(1):137–50.
[33] Mukhopadhyay SK, Ahmad MO, Swamy MNS. Compression of steganographed PPG signal with guaranteed reconstruction quality based on optimum truncation of singular values and ASCII character encoding. IEEE Trans Biomed Eng 2019;66(7):2081–90. iss.
[34] Physionet. [Online]. Available: https://archive.physionet.org/, Accessed: 2025.
[35] Banerjee S, Singh GK. A new approach of ECG steganography and prediction using deep learning. Biomed Signal Process Control 2021;64(2):1–10. iss.
[36] Kaggle. [Online]. Available: https://www.kaggle.com/datasets/bjoernjostein/shaoxing-and-ningbo-first-hospital-database?resource=download-directory, Accessed: Jul. 2025.
[37] Thomas S, Krishna A, Govind S, Sahu AK. A novel image compression method using wavelet coefficients and huffman coding. J Eng Res 2025;13(1):361–70. iss.
[38] Zigel Y, Cohen A, Katz A. The weighted diagnostic distortion (WDD) measure for ECG signal compression. IEEE Trans Biomed Eng 2000;47(11):1422–30. iss.
[39] Gupta A, Ray KC. An efficient method for detection and localization of myocardial infarction using Ramanujan Sums Wavelet Transform and Machine Learning Framework. IEEE Trans Instrum Meas 2025;74:1–13. ASN. 4005410.
[40] Hemalatha J, Sekar M, Kumar C, Gutub A, Sahu AK. Towards improving the performance of blind image steganalyzer using third-order SPAM features and ensemble classifier. J Inf Secur Appl 2023;76(5):1–10. iss.